A chemically-induced attenuated strain of *Candida albicans* generates robust protective immune responses and prevents systemic candidiasis development

Swagata Bose[1], Satya Ranjan Sahu[1], Abinash Dutta[1], and Narottam Acharya[1,*]

[1]Department of Infectious Disease Biology, Institute of Life Sciences, Bhubaneswar-751023, India.

*Correspondence to:
Narottam Acharya, Phone: 91-674-2304278, Fax: 91-674-230 0728
E-mail: narottam_acharya@ils.res.in; narottam74@gmail.com

Running title: Whole-cell Vaccine against *Candida*

Keywords: *Candida*, Candidemia, Virulence, Vaccine, Whole-cell vaccine, Cytokine, Chemokine, Nutritional Immunity,

Abbreviations: EDTA: Ethylenediaminetetraacetic acid**;** CAET: EDTA-treated *C. albicans*; *Ca*: untreated/raw *C. albicans*; DTPA: Diethylene triamine pentaacetic acid; TPEN: *N*,*N*=,*N*=-tetrakis(2-pyridylmethyl)ethane-1,2-diamine; CE: Ciclopirox ethanolamine, CFU: Colony forming units;

Abstract

Despite current antifungal therapy, invasive candidiasis causes >40% mortality in immunocompromised individuals. Therefore, developing an antifungal vaccine is a priority. Here, we could for the first time successfully attenuate the virulence of *Candida albicans* by treating it with a fungistatic dosage of EDTA and demonstrate it to be a potential live whole cell vaccine by using murine models of systemic candidiasis. EDTA inhibited the growth and biofilm formation of *C. albicans*. RNA-seq analyses of EDTA-treated cells (CAET) revealed that genes mostly involved in metal homeostasis and ribosome biogenesis were up- and down-regulated, respectively. Consequently, a bulky cell wall with elevated levels of mannan and β-glucan, and reduced levels of total monosomes and polysomes were observed. CAET was eliminated faster than the untreated strain (*Ca*) as found by differential fungal burden in the vital organs of the mice. Higher monocytes, granulocytes, and platelet counts were detected in *Ca- vs* CAET-challenged mice. While hyper-inflammation and immunosuppression caused the killing of *Ca*-challenged mice, a critical balance of pro- and anti-inflammatory cytokines-mediated immune responses are the likely reasons for the protective immunity in CAET-infected mice.

Introduction

Candida species colonizes several anatomical niches of a host, either as a commensal or opportunistic fungal pathogen. Infections by *Candida* sp. range from superficial oral and vulvovaginal candidiasis (VVC) to serious invasive candidiasis[1,2]. In immunosuppressed conditions, these fungi can evade subsided mucosal immunity and disseminate into the bloodstream, resulting in systemic candidiasis with a mortality rate of >40%. *Candida albicans* is the frequently isolated species responsible for the majority of these infections, thus, imposing a huge threat to human health worldwide. Currently, polyenes, echinocandins, and azoles are the three major classes of antifungals available to combat fungal diseases[3,4]. These drugs are characterized by a narrow spectrum of activity to target limited fungal species and often exhibit cytotoxicity to cause side effects. Over 1.5 million yearly global burdens of lethal infections suggest that the treatment of fungal diseases by using available antifungal drugs seems to be partially helping, and additionally, the emergence of drug-resistant isolates clearly emphasize the urgent need of better diagnostics, safe and broad-spectrum novel antifungal drugs, and effective immunotherapeutics and prophylactics[5]. Since no approved vaccine is available for human use, designing and developing vaccines against fungal pathogens is a priority[6]. NDV-3A and PEV7 are two recombinant vaccines that seem to be protecting recurrent VVC during initial human clinical trials[7,8]. In addition, various studies on host-fungal interactions have helped to identify multiple experimental vaccine candidates and those were shown to be safe and effective in animal models[6]. Most of these are suggested to generate neutralizing antibodies and are expected to be effective against *Candida* infections. The interaction between the host immunity and fungal pathogens is very complex and varies depending upon the nature and site of infections, and there are at least three layers of immune responses operating simultaneously against the invaders: innate, adaptive, and trained[9,10]. Also, as *C. albicans* is a multimorphic fungus, designing and developing a whole-cell vaccine approach seems to be arguably ideal.

Whole-cell vaccines can be either live or killed, and both kinds of vaccines are effectively in use against viral and bacterial infections. Heat-killed *C. albicans* and *Saccharomyces cerevisiae* strains were found to be partially protecting against experimental vaginal candidiasis[11,12]. Some of the genetically engineered *C. albicans* strains (tet-NRG1, PCA-2, CM1613, etc.) were reported to be attenuated and protective against disseminated candidiasis in mice[6,13]. However, clinical trials for these strains are yet to be commenced. Since *C. albicans* co-evolves with the host and lives mostly as a beneficial gut pathogen[2], the host must be employing certain mechanisms to block its transition to a pathogenic trait which can be explored to develop attenuated strains of *C. albicans* naturally rather than using a recombinant DNA technology approach. “Nutritional immunity” is one such frontline defense mechanism that limits fungal growth and pathogenesis[14].

Metals play a pivotal role in host-pathogen interaction. Metals like iron, zinc, manganese, magnesium, copper, etc. being a cofactor of various metabolic and non-metabolic enzymes are essential for both host and pathogens. Therefore, excessive or limited availability of metals is deleterious to cells. Several studies suggest that the virulence and pathogenesis of fungi require a threshold level of these metals[15,16]. To starve pathogens of essential metals, the host organism employs nutritional immunity strategies to reduce the availability of metals, thereby the virulence and disease progression of a pathogen is suppressed drastically[17-19]. Our recent report found that a soluble factor released from *E. coli* during co-culturing inhibited the growth, biofilm formation, and morphological transition from yeast to hyphae of *C. albicans*[20]. In an animal model, the culture supernatant of *E. coli* attenuated the virulence of *C. albicans* significantly. Chemical complementation analyses revealed that the exogenous addition of divalent metals rescued the growth of *C. albicans* which was inhibited by *E. coli*[20]. Based on the concept of nutritional immunity and these reports, we argued that the metal chelators like EDTA, DTPA, etc. could mimic *E. coli in vitro* to regulate the virulence and pathogenesis of *C. albicans*. Live whole-cell vaccine strains are generated mainly by genetic manipulation, here, we developed and characterized for the first time a chemical reagent-based attenuated strain of *C. albicans* which is safe and effectively protects systemic candidiasis in a pre-clinical model.

Results

Metal chelators inhibit the growth and biofilm of *C. albicans*

To begin with, the effect of a range of concentrations of EDTA (0.9 - 500 μM) on the growth of *C. albicans* was determined by measuring the optical density (OD_{600nm}) of the culture in the presence of the reagent. Although we observed significant growth retardation of *C. albicans* at 125 μM EDTA, upon addition of 250 μM EDTA, the growth was inhibited completely and remained saturated beyond this concentration. This result was also validated on solid YPD media where no colony formed at the highest dilution of the spot when the *C. albicans* was treated with 250 μM EDTA (**Fig. S1 A-C**). Henceforth, 250 μM EDTA was used for subsequent analyses. To determine the effect of EDTA on the survivability of fungal cells, *C. albicans* cells (OD_{600nm}= 0.5 or 10^7 cells per mL) in YPD media were grown for 12 hrs without and with 250 μM of the metal chelator. At various time intervals, an equal number of cells were harvested and stained with SYTOX Green and propidium iodide (PI), and analyzed by flow cytometry and microscopy, respectively (**Fig. S2 A-D**). Both analyses suggested that 250 μM EDTA had minimal effect on the survivability of *C. albicans* cells during this period of growth as an equal percentage of dead cells were detected in untreated as well as treated conditions. Thus, the inhibitory effect of 250 μM EDTA on the growth of *C. albicans* cells is not due to the accumulation of dead cells but rather due to the

slowing down of the cell division process. To further characterize the effect of EDTA, we checked various morphological forms of *C. albicans* upon exposure to 250 μM EDTA and 10% serum (**Fig. S3 A - C**). *C. albicans* exists predominantly in the round form under normal physiological conditions; however, in the presence of inducers like serum, it transits into its reversible forms such as pseudohyphal and hyphal forms. Our results revealed that the 250 μM EDTA treatment did not alter the morphology of *C. albicans* cells and it minimally affected the morphological switch induced by serum. Even the germ tube length induced by serum was barely affected by the addition of EDTA.

Since EDTA inhibited the *C. albicans* growth, to identify the metals that could effectually rescue *C. albicans* survival, we supplemented various divalent metal salts to the EDTA-treated *C. albicans* cells (**Fig. 1 A and B**). Both the growth curve and CFU analyses revealed that the antagonizing effect of 250 μM EDTA on *C. albicans* was abolished by supplementing with metals like $MgSO_4$, $MnCl_2$, $FeCl_2$, and $ZnCl_2$. Since the number of colonies remained the same for 8 – 24 hrs of treatment with EDTA, it again suggested that EDTA most likely is a fungistatic inhibitor whose effect can be reversed by divalent metal complementation. To further strengthen the result, $MgSO_4$ was supplemented to the EDTA treated culture at 6 hrs post-treatment rather than at 0 hr and growth was allowed. Interestingly, the suppressed growth of EDTA-treated *C. albicans* cells was rescued significantly and the effect 250 μM EDTA was minimized even in this context. Interestingly, the exogenous addition of these metals (8 μM) alone to the YPD media had no or minimal effect on the growth of *C. albicans*.

To strengthen the result, the effect of EDTA and metals on the preformed biofilm of *C. albicans* was determined (**Fig. 1 C and D**). Consistent with the growth curve result, EDTA inhibited the biofilm of *C. albicans* but was rescued by the addition of divalent metals. To substantiate the inhibitory role of EDTA, the effect of four more metal chelators Diethylene triamine pentaacetic acid (DTPA), *N*,*N*=,*N*=-tetrakis(2-pyridylmethyl)ethane-1,2-diamine (TPEN), Aprotinin, and Ciclopirox ethanolamine (CE) on *C. albicans* growth was determined. DTPA is an aminopolycarboxylic acid consisting of a diethylenetriamine backbone with five carboxymethyl groups, and has a high affinity for di- and tri-metal cations[21]. TPEN is an intracellular membrane-permeable ion chelator of transition metals[22]. CE acts by binding to and chelating trivalent cations mainly iron[23]. Unlike these chelators, BPTI or aprotinin is an antimicrobial peptide that lowers the cellular levels of magnesium[24]. Growth curve, CFU analysis, and biofilm formation assays revealed that all of these metal chelators inhibited the growth phenotypes of *C. albicans* with varied efficiency (**Fig. 1 E-H**). While the effect of DTPA and aprotinin was very similar to EDTA; TPEN, and CE inhibited both growth and biofilm of *C. albicans* drastically even at a lower concentration (100 μM) and accordingly, hardly any colony formed on solid YPD plates, and poor biofilm was observed. These results suggested that essential metals like magnesium, manganese, iron, and

zinc are required for the growth and biofilm development of *C. albicans,* and sequestration of these by a range of metal chelators affects the growth of *C. albicans.*

Global transcriptomic changes of *C. albicans* in response to EDTA treatment

Next, we investigated any changes in *C. albicans* gene expression due to EDTA treatment using high-throughput RNA sequencing. To achieve our goal, total RNA isolated from *C. albicans* cells grown for 6 hrs without or with 250 μM EDTA treatment was subjected to RNA sequencing using an Illumina NovaSeq platform, and a summary of reads obtained from each sample and their mapping to the reference genome is given in **Table-1**. On average, we obtained 19,190,581 reads per sample with 98 % or more successfully mapping to the known mRNA in the *C. albicans* strain SC5314 reference genome (assembly ASM18296v3). Principal-component analysis (PCA) was conducted to provide a pictorial representation of the transcriptomic similarities among various triplicates and it revealed that the EDTA-treated *C. albicans* samples clustered separately from the untreated ones, indicating a high level of correlation among samples with distinct transcriptome profiles (**Fig. S4A**). The total differentially expressed genes in untreated and EDTA-treated *C. albicans* cells (here onwards it will be named as *Ca* and CAET, respectively) were 5915, of these, 3093 and 2822 genes were up and downregulated, respectively. So, our RNA sequencing data indicated that EDTA has a profound effect on *C. albicans* gene expression resulting in alterations in the transcriptome. In order to find genes that were significantly dysregulated, two cut-offs: (1) false discovery rate (FDR) cut-off ≤ 0.05 and (2) log2 fold change (FC) cut-off ≥ 1 were applied; and a total of 799 differentially expressed genes (DEGs), of which 411 were upregulated and 388 were downregulated in CAET. The volcano plot depicted two pools of genes that are significantly up- (red dots) and down – (blue dots) regulated in CAET (**Fig. 2A**). The hierarchical clustering algorithm was used to create a heat map by taking top 25 up- and 25 down-regulated DEGs (**Fig. 2B**). The heat map suggested a minimal variation in cluster linkage among similar samples and thus, the dysregulated DEGs upon treatment with EDTA relative to the untreated controls were consistently observed. We re-verified the RNA seq results by carrying out real-time and semi-quantitative PCR analyses of representative genes. Upregulation of *ZRT1, CHT4*, and *PGA13*, and downregulation of *ACO2, PLB1*, and *THI13* genes were observed in CAET in comparison to *Ca* (**Fig. S4B**).

Treatment with EDTA upregulates the expression of *C. albicans* genes required mainly in metal transport and pathogenesis

In the analysis of the top 100 upregulated genes those expressions varied >5 folds higher in response to EDTA (**Table-2, Fig. 2C**), about 57 % of uncharacterized genes with unknown functions emerged. Interestingly, the function of 6 out of 12 top most upregulated genes that were >30 folds more expressed

in treated than the untreated *C. albicans* cells are yet to be deciphered. UniProt only predicts the following uncharacterized proteins CAALFM_C200860CA (orf19.9586 may encode a leucine-rich repeat protein of 418 aa with protein kinase binding function), CAALFM_C401340WA (orf19.12123 may encode a secreted protein of 109 aa), CAALFM_CR08740WA (orf19.13808 may encode a SWIM-type domain-containing protein of 226 aa), CAALFM_CR02340WA (orf19.11220 may encode a vacuolar protein sorting-associated protein 8 homolog of 419 aa), CAALFM_CR07740WA (orf19.2633.1 may encode a Histone H2B protein of 64 aa), and CAALFM_C602100WA (orf19.10993/*LDG8* may encode a cell wall protein of 167 aa) **(Table-S1)**. We found 13 DEGs related to metal transport and homeostasis, 15 DEGs of cell wall and membrane-associated proteins other than functions related to metals, and another 15 DEGS of diverged functions. The characterized top 6 upregulated genes with >30 folds higher expression were *ZRT1* (zinc ion transmembrane transported required for zinc sequestration), *PRA1* (cell surface protein involved in zinc binding and metallopeptidase activity), *CFL5* (Ferric-chelate reductase required for iron and copper ions uptake), *CFL2* (Ferric-chelate reductase required for iron and copper ions uptake), *PHO87* (SPX domain-containing inorganic phosphate transporter), and *ZRT2* (zinc ion transmembrane transporter activity) having roles in zinc, iron, and phosphate transportation[18,25,26]. In the category of <30 but > ~5 folds higher expressed genes, 51 uncharacterized genes, 7 genes (*CSA1, CSA2, CSR1, HAP3, CFL4, FRE9,* and *ARH2*) having a role in essential metal transport and homeostasis, 15 cell wall and plasma membrane-associated genes (*SCW4, PGA13, PGA31, CHT4, RIM9, ALS4, CSH1, MRV8, HGT5, CDA2, PRN4, GLX3, PGA7, RBT5,* and *JEN1*), and 15 genes (*LAP3, IFD6, ATO1, NOP6, RAS2, HST6, STE23, FGR46, POL93, HPD1, AOX2, SOU2, GPD1, CAG1,* and *FDH1*) with other function. More importantly, according to earlier studies, 24 of these upregulated genes were shown to be associated with fungal virulence, thus, EDTA-treated *C. albicans* cells might exhibit differential pathogenicity[15,25,27,28].

Further, GO annotation analyses of all 411 upregulated genes revealed a total of 37 GO terms (28 biological processes (BP), 5 molecular functions (MF), and 4 cellular components (CC) that were enriched upon EDTA treatment (**Table-S2 A, Fig. 2E**). The highly significant upregulated biological processes GO terms were oxidation-reduction (GO:0055114), inter-species interaction (GO:0044419), pathogenesis (GO:0009405), and transition metal transporters and utilization (GO:0006812, GO:0048878, GO:0019725, GO:0098771, etc.). Similarly, GO terms of molecular function (GO:0098771, GO:0016616, etc.) genes encode for enzymes required for oxidation-reduction reactions, and GO terms of cellular component (GO:0071944, GO:0005886, etc.) mostly indicate upregulated genes belong to the cell wall and its periphery. To find out the gene networks that were affected upon EDTA treatment, STRING (Search Tool for the Retrieval of Interacting Genes/Proteins) analysis was carried out (**Table- S3 A**).

High confidence (0.7 confidence level) analysis revealed upregulation of network proteins mostly involved in metal ion transport and 18 strong nodes were detected among 15 out of 31 genes **(Fig. 2G)**. Another gene network of 33 genes that caught our attention involved in pathogenesis and 9 DEGs of this network are directly or indirectly shown to be involved in fungal pathogenesis **(Table-S4, Fig. 2H).** Altogether, our analysis suggested that the upregulation of cell wall and plasma membrane-associated genes whose products mostly play a role in metal transport and utilization and in pathogenesis (or survival in the host) occurred in response to EDTA. This could indicate a compensatory mechanism being utilized by *C. albicans* in an attempt to overcome essential metal scarcity due to EDTA treatment.

Treatment with EDTA results mostly in downregulation of genes associated with ribosome biogenesis and One-carbon metabolism in *C. albicans*

Similar to upregulated genes analyses, the top 100 downregulated genes those expression reduced to 3-100 folds in response to EDTA treatment (**Table-3, Fig. 2D**), and 25 uncharacterized genes with unknown functions emerged. Seven of these genes CAALFM_C404230WA (orf19.9003 may encode an MFS domain-containing membrane protein), CAALFM_C112940CA (orf19.4923.1 may encode a rod shape-determining protein MreC), CAALFM_CR09350CA (orf19.7330 may encode TENA_THI-4 domain-containing protein), CAALFM_CR06430WA (orf19.8344 may encode a mediator of RNA polymerase II transcription subunit 7), CAALFM_CR08830WA (orf19.7279.1 may encode a mitochondrial ATP synthase-coupling factor 6), CAALFM_C106870CA (orf19.6222.1 may encode a thyroglobulin type-1 domain-containing protein) and CAALFM_C400530CA (orf19.11666 may encode a SurE domain-containing protein) exhibited minimum of 5 folds reduced expression in CAET (**Table-S5**). We observed downregulation of 44 genes having roles in metabolic processes e.g. *PHO100* (Putative inducible acid phosphatase), *PLB1* (Phospholipase B), *THI4* (Thiamine biosynthetic enzyme precursor), *THI13* (Thiamin pyrimidine synthase), *GIT1* (Glycerophosphoinositol permease), *PUT1* (proline oxidase), *INO1*(inositol 1-phosphate synthase), *PUT2* (delta-1-pyrroline-5-carboxylate dehydrogenase), *LYS22* (Homocitrate synthase), *ACO2* (aconitate hydratase 2), *SNZ1* (pyridoxine (vitamin B6) biosynthetic enzyme), *BTA1*(betaine lipid synthase), *LYS4* (Homoaconitase), etc., 13 genes having roles in ribosome biogenesis and function such as *RDN18, RBT7, RPS42, RPS28B,* etc; and 7 genes encoding for cell wall/ membrane-associated proteins (*HSP30, TRY6, PGA10, HGT2, OPT1, OPT3, HXT5*).

The GO annotation analyses of all 388 downregulated genes revealed a total of 99 GO terms (64 biological processes, 12 molecular functions, and 23 cellular components) enriched upon EDTA treatment (**Table- S2 B, Fig. 2F**). The highly significant downregulated biological processes GO terms are cellular and metabolic processes mostly involved in protein synthesis, ribosome biogenesis, and amino acid

biosynthesis (GO:0009987, GO:0008152, GO:0006518, GO:0006412 etc.). Similarly, GO terms of molecular function (GO:1901363, GO:0003735, GO:0003676, etc.) genes encode for heterocyclic compounds binding, ribosome structural components, and RNA binding proteins; and GO terms of cellular component (GO:0110165, GO:0005737, GO:0005739, etc.) mostly indicate downregulated genes belong to cytoplasmic and mitochondrial components. To find out the gene networks that were inhibited upon EDTA treatment, STRING analysis was carried out (**Table- S3 B**). High confidence (0.7 confidence level) analysis revealed the downregulation of network proteins mostly involved in cytosolic and mitochondrial ribosomal proteins and one-carbon metabolism **(Fig. 2 I, J and Fig, S4 C iii)**. The cytoplasmic gene network involved in protein translation showed strong nodes between 74 genes, out of which 30, 31, and 13 DEGs belonged to 40S, 60S, and other related functions of translation **(Table-S3 C, Fig. 2 I, Fig. S4 C i and ii)**. Similarly, a network of 56 genes involved in the mitochondrial ribosome and translation components was observed to be suppressed **(Fig. 2 J)**. Interestingly, ribosome structure and stability require a high concentration of divalent metals. Another network of 34 down-regulated genes involved in one-carbon metabolism was detected (*LYS2, GCV2, ARG5, ARO8, CHA1, ARO3, ASN1, LEU42, LYS9, HIS4, AAT22, ILV6, TRP5, GDH3, PUT1, ILV5, GCV1, ARG1, ARO2, ARO4, MET6, SAH1, ARG4, MIS11, LYS22, SER2, DFR1, LYS4, LYS12, LEU4, ECM42, ILV3, PUT2,* and *GCV3)* and most of these enzymes also require divalent metals as cofactor for their activities[29] (**Fig. S4 C iii**). One-carbon (1C) metabolism is critical to support cellular processes like purines and thymidine biosynthesis, amino acid homeostasis (glycine, serine, and methionine), etc. Since the functions of ribosomes and 1C metabolic enzymes require various essential metals[30], due to scarcity of those upon EDTA treatment, cells might have evolved a strategy to lower the ribosomal activity and metabolism by reducing ribosome and polysome composition both in cytosol and mitochondria and down-regulating essential metabolic enzymes, respectively. This might have caused a delay in cell division process while the cells maintain to survive in response to EDTA.

EDTA alters the cell wall structure and composition

Since the cell wall and cell membrane components were upregulated and cytosolic biological processes were suppressed upon EDTA treatment, we examined any effect of EDTA on the ultrastructure of *C. albicans* cells by transmission electron microscopy. While the untreated *C. albicans* cells were oval-shaped, the EDTA-treated cells were mostly round-shaped with thicker cell walls (**Fig. 3A**). The thickness of the cell wall of EDTA-treated *C. albicans* cells was estimated to be 435.023 ± 22.3nm (~400-600nm) which is ~4 folds more than that of untreated (113 ± 31 nm, range of ~70-140 nm). To rationalize the elevated thickness of the cell wall in CAET, the composition of the fungal cell wall was verified. The cell wall of *C. albicans* is composed of an inner layer of chitin, a middle layer of β-glucans, and an

outermost layer of mannan[31]. These cell wall components were estimated by staining the cells with Calcofluor white (CFW), aniline blue, and Concanavalin A tetramethylrhodamine dyes, respectively, and analyzed further by flow cytometry (**Fig. 3 B-D**). Our FACS analyses suggested that these components were increased by ~0.5 to 2.5 folds when the *C. albicans* cells were exposed to EDTA, amongst mannan was the most deposited. The perfectly round shape structure of EDTA-treated *C. albicans* cells could be due to increased chitin and glucan content as they provide rigidity to the fungal cell wall and could help cells to withstand the metal scarcity associated stress.

Reduced level of total ribosomes in EDTA-treated *C. albicans* cells

Metal ions stabilize the secondary structure of rRNA, the association of ribosomal proteins to the ribosome, and the assembly of ribosomal subunits. Thereby, they are essential for maintaining the overall structure and translation activity of the ribosome[30,32]. On the other hand, ribosomes are equally important to maintain the cellular homeostasis of metal ions. Since we found a reduction in the RNA content of ribosomal and protein metabolism components upon treatment with EDTA, we intended to estimate the total ribosomes of *C. albicans* without and with 250 μM EDTA treatment. An equal amount of exponentially grown cells of two different concentrations were processed to isolate ribosomes by sucrose density gradient centrifugation and analyzed as described before[33]. A clear separation of all four different forms of ribosomes: 40S, 60S, 80S, and polysome was observed in the fractionations of both EDTA-treated and untreated cells (**Fig. 3E**). The presence of higher amount of cell-free monosomes and polysomes indicated active protein translation in the cells. Interestingly, EDTA-treated cells possessed lesser volumes of 40S, 60S, 80S, and polysome fractions than those found in untreated *C. albicans* cells.

EDTA-treated *C. albicans* cells interacted efficiently with macrophages

Innate immune cells are the first line of defense against any invading pathogens[34]. The immune cells like macrophages and neutrophils engulf *C. albicans* cells and produce reactive chemicals to eliminate the pathogen. As a counteractive measure, the fungal cells produce several enzymes and toxins to kill the host's cells and evade the immune system. Since the cell wall is the first interacting interface between the fungal and host cells, the altered cell wall composition could alter the recognition and phagocytosis of fungal cells by macrophages. To examine and compare fungal uptake and clearance by macrophages, we co-cultured differentially stained murine macrophages (RAW 264.7 cells stained with deep red) and untreated or EDTA-treated *C. albicans* cells (stained CFSE) in a 1:1 ratio and cells were taken out at different time points (1-3 hrs) for flow cytometry analysis. A gating strategy to separate unstained and deep red stained cells during fluorescence acquisition in a flow cytometer and their analyses are depicted **(Figure 4A i and ii and Fig. S4 D).** Our FACS analysis of co-cultured cells revealed that within 1-3 hrs of co-culturing, about ~78-90% of the macrophages were double-positive suggesting efficient uptake of

fungal cells by the macrophages, which is equivalent to earlier reported phagocytosis efficiency[35]. However, a comparatively lower percentage of RAW cells was found to be interacting with CAET than untreated *C. albicans* cells (~60% to 90%). At an initial time point of incubation (1 hr), macrophages engulfed untreated and treated fungal cells with equal efficiency (~90%), however, phagocytosis reduced significantly at 3 hrs in the case of CAET than *Ca* (~78 to 61%). To further validate it, internalized fungal cells were retrieved from the macrophages, and their survival was estimated by counting colony forming units (**Figure 4B i and ii**). The CFU analysis revealed more killing of CAET cells than *Ca* by macrophages upon longer co-incubation. This result indicated a faster clearance of metals-deprived condition grown *C. albicans* cells by macrophages. Similarly, PI staining of the co-cultured cells further confirmed more killing of macrophages when they interacted with unexposed than EDTA-exposed fungal cells (**Figure 4C i and ii**). These results implemented that *C. albicans* cells with thickened cell walls due to EDTA exposure get recognized and eliminated faster by immune cells than the naïve wild type *C. albicans* cells *in vitro*.

EDTA-treated *C. albicans* cells exhibit attenuated virulence in mice model of systemic candidiasis and upon immunization, they efficiently protect lethal challenge of pathogenic *C. albicans*

The systemic challenge of *C. albicans* cells induces multi-organ failure in mice similar to in humans that eventually kills the host[36,37]. Since we observed a differential virulence of fungal cells when they were co-cultured with immune cells, we determined the disease-causing ability of these fungal cells *in vivo.* BALB/c mice (n=6) were injected with 5 x 10^5 fungal cells per mouse via the lateral tail vein and monitored their survival for a month (**Figure 5A**). Mice who suffered due to severe candidiasis were euthanized based on the humane endpoints. While the mice challenged with untreated *C. albicans* succumbed to infection within 8 days post-inoculation, the mice group injected with CAET survived similarly to the saline control group and did not show any sign of infections. This result suggested that upon EDTA treatment, *C. albicans* cell loses its virulence attributes and become non-pathogenic. Therefore, we argued whether animals immunized with CAET can protect against the pathogenic challenge of raw *C. albicans* cells. To validate, two groups of BALB/c mice (n=6) were immunized intravenously either by saline or by 5 x 10^5 CAET fungal cells per mouse and after 30 days, they were re-challenged with the same inoculum size of virulent form of *C. albicans* cells per mouse and their survivability was monitored. Interestingly, while the saline control sham immunized mice succumbed to fungal infections within 9 days, the CAET immunized mice were protected to the lethal re-challenge and survived till their natural death (orange *vs* brown lines). To re-validate it, the animal-challenged experiment was repeated twice on different occasions and the results were very consistent (**Fig. S5**). We further confirmed the suffering of mice due to pathogenic *C. albicans* challenge by histopathology of

PAS-stained kidney sections and CFU analyses (**Fig. 5 B and C**). The CFU analysis of the vital organs such as the kidney, liver, and spleen of killed mice groups (*Ca* and 1°Saline-2°*Ca*) confirmed the presence of heavy *C. albicans* load (**Fig. 5B**). The kidney of infected mice had a higher fungal load (~10^5 cells) than the other two organs liver and spleen (~500-1000 cells). PAS-stained cortex and medulla portion of the kidney depicted the presence of hyphal *C. albicans* cells. Our virulence-challenged analyses demonstrated that EDTA-treated *C. albicans* by altering its cell wall structure and gene expression reduces virulence potential drastically, and such strains might generate enough immune responses to protect pathogenic WT re-challenge. More importantly, although the effect of EDTA on *C. albicans* growth was reversible by the addition of metals *in vitro*, that was not the case in animals as the CAET cells were attenuated and were efficiently cleared by the host immune mechanisms as also depicted in figure 4.

EDTA-treated *C. albicans* cells replicate *in vivo* and alter circulating immune cell profiles

C. albicans has to replicate in the host to cause diseases. Systemic circulation of fungal cells leads to colonization in various organs; therefore, sepsis and septic shock due to bloodstream fungal infections are the major causes of morbidity and mortality[6,38]. Since the EDTA-treated fungal cells were nonpathogenic, it was intriguing to determine their growth and inflammation status in the host upon systemic inoculation to animals. Three groups of BALB/c mice were intravenously injected either with saline or 5 x 10^5 of untreated or EDTA-treated *C. albicans* cells per mouse. Similarly, two more vaccinated groups of mice (sham and CAET immunization) were generated and after 30 days, they were re-challenged with either saline or by WT *C. albicans*. Mice (n=5) were euthanized at various time points and various tissues were collected (**Fig. 5 D**). The proliferation status of fungal cells was determined by counting the fungal load in various organs by CFU analyses (**Fig. 5 E**). A heavy fungal load in most of the tissues except the lungs of the 3rd and 7th day post-infected mice by untreated *C. albicans* was detected (cyan). As expected, the organs of the saline groups did not possess any fungal cells. While we could not detect the presence of *C. albicans* cells in the brain, liver, lungs, and spleen of animals infected with CAET in any post-days of infection, fungal cells were recovered from the kidney only in the 3rd and 7th days of post-challenge. On the 7th day, the fungal load in the kidney was ~35-40 folds less in CAET-challenged mice (~10^4 cells, purple bar) than in *Ca* challenged mice group (~3x10^5 cells, cyan bar). Thus, the high fungal load on the 7th day post infection by untreated *C. albicans* cells could be the major reason for the tissue damage to cause death in animals by 9 to 10 days (**Fig. 5A**). As we detected a gradual increase in fungal load from the 3rd to 7th days but no or undetectable level of fungal cells after 7 days of infection in mice challenged with CAET cells, it suggested that these cells replicate but get eliminated faster from the system leading to the survival of animals. Thus, CAET cells are live and divide in the host initially but as they cannot

evade the immune system, they were gradually eliminated. More importantly, the kidney tissues of vaccinated re-challenged mice group (1° CAET 2° *Ca*) also possessed minimal fungal burden ($3x10^3$ cells) only at 7th day post infection and no detectable fungal cells beyond this time point. This result suggested a faster clearance of WT cells leading to mice survival and most likely due to a robust protective immune response generated upon CAET vaccination (**Fig. 5E**). PAS staining of kidneys further confirmed high fungal load in untreated than EDTA treated *C. albicans* cells in the 3rd and 7th day of post-infection. No fungal cells were detected in any of the mice groups challenged with CAET beyond 10 days of post-infection irrespective of WT re-challenge (**Fig. S6 A**).

Quantitative and qualitative aberrations of immune cells like neutrophils and monocytes are found to be linked to systemic candidiasis and indicate the inflammation status of the host. To get an overview of systemic levels of various immune cells upon *C. albicans* infections, the blood of different groups of mice was analyzed to determine any alterations in blood cell profile using a blood counter (**Fig. 5F and Fig. S6 B**). A noticeable increase of about 2 to 5 folds in peripheral WBC, monocytes, granulocytes (neutrophils, eosinophils, and basophils), and platelet levels but reduced RBC were observed in *Ca* infected mice in comparison to those in saline group mice in both 3rd and 7th days of post-infection. Interestingly, CAET infected mice showed mild alteration only in WBC and platelet counts in comparison to the control group. This result again confirms attenuated virulence of *C. albicans* upon EDTA treatment. The levels of lymphocytes, and other RBC-associated parameters (MCH, MCHC, and MCV) did not alter significantly and remained the same in all three groups of mice **(Fig. S6 B).**

EDTA-treated *C. albicans* cells induce balanced levels of cytokines and chemokine production

Involvement of the pattern recognition receptor (PRRs) of macrophages, dendritic cells, etc. in recognizing fungal pathogens induces multiple cytokines and chemokines, which in turn activate a cascade of host immune responses. T-cells are also the major producers and effectors of these messengers. The levels of these messengers are differed in different sites of infections and responses to the virulence status of *C. albicans*[39]. For our analysis, we estimated circulating serum cytokine and chemokine levels in virulent and avirulent fungal-challenged mice and compared them with the saline group in a time-dependent manner by using a multiplex array system (**Fig. 6**). Despite differential rates of fungal replication *in vivo*, on the 3rd day of infection, all of the tested cytokines and chemokines were induced in the fungal infected mice serum irrespective of the virulence status, although with very high level in untreated *C. albicans* inoculated mice than CAET group in comparison to that in the control suggesting a prompt triggering of early inflammatory response. While we observed a gradual decline of these towards the basal levels exclusively in mice infected with CAET from 3 to 30 days post-challenge, a

significant rise on the 7th day of *Ca*-challenged mice was evident. This upsurge might have created enough immunosuppressive as well as hyper-inflammatory environments allowing fungal propagation and systemic fungal infection leading to host tissue damage and mortality by the 9th day. Especially, Th-1 cytokines like IL-1β, IL-10, GM-CSF, Th-2 cytokines IL-4 and IL-13, and IL-17 from Th-17 type were highly induced on the 7th day of mice group infected with virulent form of *C. albicans*. Increased levels of anti-inflammatory cytokines like IL-2, IL-3, IL-4, IL-5, IL-9, IL-10, and IL-13 will cause immunosuppression, while the pro-inflammatory cytokines like IL-1, IL-12, IL-6, IL-17, IFN-γ, and TNF-α might lead to hyper inflammation in untreated *C. albicans* challenged mice. The levels of chemokines like RANTES, MCP-1, MIP-1 (α and β), KC, and EOTAXIN were also found to be high in the serum of fungal-infected mice, and similar observations were also found in the kidney and spleen tissues of infected murine in an earlier reported study[39]. Taken all together our data suggest that while a critical balance of the pro-and anti-inflammatory cytokines mediated immune responses is maintained for a long duration in mice challenged with CAET to induce antifungal protective immunity, both of these cytokines remained high in the pathogenic-challenged mice group leading to immunosuppression and death. Altogether this study found that CAET cells are live but non-pathogenic and boost immune responses to protect against lethal fungal challenges in a pre-clinical model; thus, CAET could be explored further as a potential whole-cell vaccine candidate.

Discussion

This study explored the effect of metal chelators specifically EDTA as a component of nutritional immunity on *C. albicans* biology (**Fig. 7**). Here we found that EDTA inhibits biofilm formation and the growth of *C. albicans* in both liquid and solid media. Other metal chelators like DTPA, aprotinin, TPEN, and CE also exhibited similar or more pronounced effects on *C. albicans*. The limited antifungal effect of EDTA on fungal colonization and growth by chelating calcium ions from the medium has been shown in earlier studies[40,41,42]. These chelators were also shown to synergize with antifungals like azoles and caspofungin to inhibit fungal growth and biofilm formation[43,44,23,45,46]. All these reports including ours establish the importance of metals in *C. albicans* pathogenesis. Although the antifungal property of metal chelators has been known for a while, this is the first report to explore whether EDTA or any other metal chelator can also attenuate the virulence of a fungal pathogen.

Next, we provide a comprehensive view of transcriptomic changes associated with the treatment of *C. albicans* with EDTA and their effect on fungal pathogenesis. Major changes in the expression of key genes and pathways associated with *C. albicans* were metal transport and homeostasis, pathogenesis processes, ribosome biogenesis, and one-carbon metabolic enzymes among others. While the cell wall

and membrane-associated components were upregulated, cytosolic components were downregulated upon EDTA exposure. To our surprise, only the iron (*CFL5, CFL2, CSA2, CSA1, HAP3, FRE9, ARH2, FTR1, FTR2, FET3, SIT1,* and *FTH1*,) and zinc (*ZRT1, ZRT2, CSR1, PRA1*) transporters were upregulated upon EDTA treatment, whether these genes are also involved in the transportation of other metals like magnesium, manganese, etc. require further investigation. As reported earlier *ALR1, MRS2, LPE10,* and *MNR2* are required for magnesium transport[23,47,48], however, the expression of these genes remains unaltered in our analysis. Most of these upregulated genes involved in metal homeostasis are also found to be associated with fungal virulence. For example, *PRA1* and *ZRT1* collaborate to sequester zinc and mediate endothelial damage of host cells[18]. Further study suggested that Pra1 blocks fungal immune recognition and inhibits recruitment, adhesion, and effector functions of both the host's innate and adaptive immune responses[49]. A phosphate transporter *PHO87* was also highly upregulated upon EDTA exposure suggesting phosphate starvation, and the role of phosphate metabolism in virulence was shown in the past[50]. The outer layer of the *C. albicans* cell wall is enriched in highly glycosylated proteins like the GlycosylPhosphatidylInositol (GPI)-anchored proteins (GpiPs)[51] and this study revealed upregulation of many such proteins (*PGA7, PGA13, PGA17, PGA19,* and *PGA31*). Some of these GpiPs are involved in cell wall synthesis, morphogenesis, and adhesion. Accordingly, these genes might have contributed to the increased thickness of the cell wall upon EDTA treatment by enhancing mannan, β-glucan, and chitin depositions. Consistent with this, an earlier report showed that deletion of *PGA13* caused increased sensitivity to Congo red, Calcofluor white, and zymolyase; delayed filamentation, increased adherence, and reduced virulence in a mouse model[52]. Similarly, the *pga7*ΔΔ mutant also exhibited reduced virulence in the murine model of systemic candidiais[27]. The *pga31*ΔΔ mutant shows modifications in the cell wall composition and caspofungin sensitivity[53]. EDTA treatment also enhanced the expression of a small network of well-characterized genes associated with filamentation and pathogenesis of *C. albicans* (*BRG1, TEC1, UME6, HWP1, HGC1, SAP5,* and *SAP6*). Secreted aspartyl proteinases (Saps) are encoded by a multigene family of at least nine members (*SAP1* to *SAP9*) and Sap4, Sap5, and Sap6 isoenzymes are important for the normal progression of systemic infection by *C. albicans* in animals[54]. Hwp1 is a hyphal-specific cell wall protein and its role in virulence is debatable[55,56]. *UME6* is a transcriptional regulator that is induced in response to environmental cues and the *ume6ΔΔ* mutant exhibits a defect in hyphal extension and is attenuated for virulence in animal model[57]. *HGC1* is a hypha-specific G1 cyclin-related protein involved in hyphal transition and virulence[28]. Transcription factors like Bcr1, Brg1, Rob1, Hgc1, and Tec1 were shown to be involved in biofilm formation as loss of any one of these regulators significantly compromised biofilm formation both *in vitro*, and *in vivo*[58]. Contrary to all these reports, despite the upregulation of these virulence genes, our study showed EDTA inhibiting biofilm formation of *C. albicans in vitro* and virulence in cellular and animal models. Among the down-regulated genes,

genes of the ribosome biogenesis and one carbon metabolic process stood out. Altogether, our transcriptomics analysis suggested that due to the scarcity of essential metals upon EDTA treatment, *C. albicans* induced its metal uptake ability by expressing various transporters and increased the efficiency of the cell wall and membrane components, at the same time; it reduced the cytosolic activity to a bare minimum by down regulating ribosomal and 1C metabolic genes to withstand metal deficiency and that likely induced a dormant-like state in *C. albicans*.

Although some of the virulence genes were upregulated upon EDTA treatment and their specific deletions are known to cause attenuated virulence in animal models, CAET cells were eliminated faster by macrophages and became avirulent in mice. It emphasizes that the virulence of *C. albicans* is very complex and multifactorial, and requires a network protein to manifest candidiasis development. In this study downregulation of ribosome biogenesis and metabolic enzyme synthesis seem to be the predominant factor in suppressing the virulence of *C. albicans*, whereas the overexpression of cell wall-associated virulence genes might have played a role in enhancing recognition by the immune cells and host immune responses. Unlike untreated *C. albicans* which multiplies in the host rapidly and the count reaches the maximum (>10^5 CFU/kidney) at day-7 in most of the essential organs causing tissue damage and death on the 9th -10th day, the CAET cells multiplied very slowly in infected organs (<10^4 CFU/kidney at 7th day) and were eventually cleared from the system by the 10th day. Host defense against systemic *Candida* infection depends mostly on the efficacy of phagocytosis of fungal cells by innate immune cells. This study showed an increased number of monocytes, granulocytes, and platelets in the circulation of mice infected with *Ca* than in CAET. This also suggests differential virulence properties of these two fungal strains. The fungal cell wall is the first point of contact with the innate immune system and plays an important role in recognition by neutrophils and macrophages. β-glucan of *C. albicans* cell wall is recognized by dectin-1/ Toll-like receptor-2 (TLR2) receptor as the major PAMPs that trigger both host protective immunity and pathogenic inflammatory responses. The mannose receptor (MR) and TLR4 recognize N-linked and O-linked mannans, respectively[9]. The thick cell wall of CAET contained a higher proportion of all the components, and these constituents probably played a key role in efficient phagocytosis and clearance by the macrophages than the untreated *C. albicans* cells.

Cytokines and chemokines play important roles in regulating inflammation and immune activation due to the presence of a pathogen. To analyse differential cytokines-mediated immune responses in infected mice, 16 cytokines and 6 chemokines from the serum were estimated. Induction of anti- and pro- inflammatory cytokines by the pathogenic *C. albicans* as early as 3-7 days post-infection might have caused immune suppression, hyper inflammation, and tissue damage promoting excessive fungal growth, sepsis, and death of the mice within 10 days. However, in CAET-infected mice, a critical balance of pro- and anti-inflammatory cytokines was developed. Both pro- and anti-inflammatory

cytokines and chemokines levels gradually decreased from the 3rd day to 30th day, but a critical level above basal was still maintained to provide protective immunity, thus by immunization with CAET, animals were protected from the lethal challenge of *C. albicans*.

Differential levels of cytokine induction in untreated *Vs* EDTA-treated *C. albicans* infected mice again suggested possible involvement of T- cells as they are the major producers and effectors of these messengers. The protective immunity against fungal pathogens is mostly dependent on the balanced activation of 'protective' Th-1 and 'non-protective' Th-2 responses[9]. Fungal infections inducing the Th-1 cytokines (e.g. IFN-γ, TNF-α, and IL-2) in the serum of infected individuals have been reported and these are involved in macrophage activation, nitric oxide production, and cytotoxic T lymphocytes proliferation to enhance phagocytosis and fungal clearance[9]. IFNγ is central to anti-fungal resistance against systemic candidiasis as the IFNγ knockout mice are highly susceptible to disseminated *C. albicans* infection[59]. IL-12 acts on NK and T cells to produce IFN-γ which in turn stimulates monocytes and macrophages to produce IL-12. Deficiency of IL-12 or IL-12R genes leads to enhanced fungal infections. The Th-2/Th-17 cytokines IL-4, IL-5, IL6, IL9, IL-13, and IL17 levels also increased in the serum of fungal-challenged mice. IL-4, IL-5 and IL-13 are responsible for the production of non-opsonizing antibodies, allergic reactions, and the suppression of inflammatory reactions caused by Th1 cytokines. Exogenous supplementation of recombinant IL-4 to mice increases susceptibility to invasive fungal infections, again suggesting the deleterious effects of Th2 responses[60]. IL-6-deficient mice are more susceptible to invasive candidiasis than wild type mice, which suggests that IL-6 release is fundamental during fungal infection and the severity of sepsis. Th17-response results in the production of IL-17, IL-21, and IL-22 cytokines. IL-17 upregulates several chemokines and matrix metalloproteases through the NF-κB and MAPK signalling pathways, leading to the recruitment of neutrophils into the sites of inflammation during fungal infections[10,61]. Not surprisingly, IL-17R null mice are highly susceptible to systemic candidiasis[62]. Other cytokines such as TNF-α, IL-6, and GM-CSF are also involved in neutrophil recruitment during candidiasis. From the cytokine profiling it is evident that while an optimal balance between Th-1 and Th-2/Th-17 responses seems to be maintained in CAET-challenged mice, an increased levels of these was observed in *Ca*-challenged mice. Chemokines are also critical for immune cell trafficking during pathogen attack and are released at an early stage of fungal infection. They bind to their respective receptors to trigger interleukins production to promote fungal clearance[63]. This study reports higher levels of CC-type chemokines (MCP-1, KC, MIP-1α, MIP-1β, RANTES, and EOTAXIN) in infected mice and follow similar trends as cytokine in *Ca vs* CAET challenged groups. Platelets are known to produce some of these immune mediators like RANTES and PF4 with antimicrobial activity against *Candida* species, and platelet-rich plasma inhibits the growth of *Candida*[64].

Apart from innate and adaptive immunity, trained immunity also seems to be critical to providing immunological memory that is dependent on epigenetic reprogramming of innate immune cells[9]. It has been suggested that the trained immunity is induced through the binding of dectin-1 to the β glucans of *C. albicans* followed by activation of the non-canonical RAF1-cAMP signaling pathway causing epigenetic imprinting through histone methylation and acetylation, thereby, it boosts pro-inflammatory cytokines production in trained monocytes and macrophages. As the EDTA-treated *C. albicans* cells have a high level of β glucans and upon its immunization, the animals were protected to the the lethal re-challenge of WT strain, the role of trained immunity cannot be ruled out. A detailed cellular and molecular mechanisms underlying protective immune responses in CAET challenged mice require further investigation and are awaited. Nevertheless, based on the presented results, CAET has the potential to be developed as a live whole-cell vaccine against fungal infections.

Materials and Methods

Animal Ethical clearance: Mice and protocols involving animals were approved by the Institutional Animal Ethical Committee, Institute of Life Sciences, Bhubaneswar, India, with a Permit Number ILS/IAEC-133-AH/AUG-18. The mice experiments were conducted following the guidelines of the institute.

Animal, strains, and growth conditions: BALB/c female mice of 6-8 weeks old were procured from the institute animal house and maintained in individually ventilated cages under the standard condition with ad libitum. *C. albicans* (SC5314) strain was cultivated in YPD nutrient media. The yeast cells were stocked in 30 % glycerol and kept at -80 °C for longer storage. For all experiments, *C. albicans* pre-culture was made by growing cells for 16-18 hrs in YPD growth media at 30 °C with continuous shaking at 200 rpm.

Identification of fungistatic concentration of EDTA: To determine the fungistatic concentration of EDTA, the pre-culture of *C. albicans* was diluted to an OD_{600nm}=0.5 (10^7 cells per mL) in fresh YPD media. Serial dilutions of EDTA concentration were prepared in a 96-well plate by using YPD media across multiple wells to obtain a gradient ranging from 500µM to 0.9µM with a total volume of 150 µL in each well. Following the setup, 2 µL of the diluted *C. albicans* culture was added to each well. A positive control (represented as 0 µM) comprising of *C. albicans* culture alone and a negative control containing YPD only were also prepared. The plate was incubated at 30 °C under a static condition for 24 hrs. The optical density at 600nm of the growth was measured using a Perkin-Elmer plate reader. The experiment was performed with four technical replicates. Further, certain concentrations of EDTA treated cells post-24 hr treatment (0-250 µM) were selected from the 96-well plate and their respective dilutions were

spotted on the YPD agar plate to determine the viability of the *C. albicans* cells. The plate was incubated at 30 °C for 24 hrs and imaged.

Growth curve and CFU analysis: The overnight *C. albicans* pre-culture was diluted to an OD_{600nm}=0.5 in YPD media, with each tube containing a final volume of 10 ml. Except one, these cultures were treated individually with 8 µM $MgSO_4$, 8 µM $ZnCl_2$, 8 µM $FeCl_2$, 8 µM $MnCl_2$, 250 µM EDTA + 8 µM $MgSO_4$, 250 µM EDTA + 8µM $ZnCl_2$, 250 µM EDTA + 8 µM $FeCl_2$, and 250 µM EDTA + 8 µM $MnCl_2$. Similarly, the metal chelators used for the other analyses were 250 µM DTPA/pentetic acid, 250 µM BPTI/Aprotinin, 100 µM TPEN, and 100 µM CE. Over the next 24 hrs, the OD_{600nm} and colony forming unit efficiency of the untreated and treated cultures were monitored. For CFU analysis, the cultures were serially diluted in autoclaved distilled water and around 100-150 µl of diluted samples were spread onto the YPD agar plates. The plates were incubated, colonies calculated, and the graph was plotted against time using Graph Pad Prism version 8.0. A similar growth curve and CFU analyses of *C. albicans* culture were also carried out in the presence of 250 µM EDTA, and 8 µM $MgSO_4$ was supplemented after 6 hrs of treatment. The experiment was repeated thrice with biological duplicates.

Estimation of cytotoxic effect of 250 µM EDTA on *C. albicans* cells using SYTOX green and PI staining: In order to compare the viability of *C. albicans* cells in untreated and EDTA treated condition, *C. albicans* cells (OD_{600nm}=0.5) were grown without and with 250 µM EDTA at 30 °C and 200 rpm for 12 hrs. An equal volume of cells were harvested at various time intervals, and washed two times and resuspended in 1 mL 1X PBS. SYTOX green (Thermo Fischer Scientific) staining was conducted at a final concentration of 1 µg/mL, followed by a 30 mins incubation at 30 °C in the dark. Stained cells were washed and resuspended in 500 µL 1X PBS and data was acquired in BD LSR Fortessa Flow cytometer with excitation by a blue laser at 488 nm. Data were analyzed using FlowJo software and were exported in the JPEG format. Similarly, another set of cell pellet was stained with propidium iodide (200 ng/mL) and images were captured using a fluorescence microscope (EVOS imaging system; Thermo Fischer Scientific). About 1000 cells were counted and the % of PI stained cells were determined. The experiment was repeated thrice with biological duplicates.

Morphology analyses

To determine the effect of 250 µM EDTA on the morphology of *C. albicans* cells, from the above grown cultures, cells were collected at various time intervals and the cellular phenotypes were observed under a 40 X Leica DM500 microscope. The percentage of singlet, doublet, pseudo-hyphae, and hyphae cells were estimated. Since serum induces germ tube formation, *C. albicans* cultures were grown in the presence of 10% serum (FBS; Gibco) and without and with 250 µM EDTA at 37 °C. Germ tube lengths

were observed under the light microscope and length was measured using ImageJ software. The experiment was repeated thrice with biological duplicates.

Biofilm formation assay

Biofilm of *C. albicans* was developed by growing diluted overnight culture in YPD broth (OD_{600nm}=0.5) in a 24-well polystyrene plate for 24 hr in a static condition at 30 °C as described before[20]. After, 24 hr of biofilm formation, the biofilms were either kept untreated or treated with 250 µM EDTA or mentioned concentrations of other metal chelators (DTPA, Aprotinin, TPEN, and CE), 8 µM $MgSO_4$, 8 µM $ZnCl_2$, 8 µM $FeCl_2$, 8 µM $MnCl_2$, 250 µM EDTA + 8 µM $MgSO_4$, 250 µM EDTA + 8 µM $ZnCl_2$, 250 µM EDTA + 8 µM $FeCl_2$, and 250 µM EDTA + 8 µM $MnCl_2$; and again, incubated for another 24 hr. After a total 48 hrs of incubation, the supernatant was gently removed without disturbing the biofilm and the wells were washed with 1X PBS twice. The biofilm so obtained was treated with 0.1% crystal violet and left for 20 minutes to stain at 25 °C. The plate was allowed to air dry and the bound dye was then re-suspended in 33% glacial acetic acid, and absorbance was recorded at 570 nm using a Perkin-Elmer plate reader. The experiments were repeated twice with biological triplicates. Similarly, biofilms were formed and treated in 8 well-chambered slides, images were obtained after staining with 1% acridine orange using Leica TCS SP8 confocal scanning system with where excitation at 483 nm and emission with 500 to 510nm band-pass filter were used.

RNA extraction and sequencing: The pre-culture of *C. albicans* was diluted to an OD_{600nm}=0.5 (10^7 cells per mL) in 5 ml of YPD media. The culture was treated with 250 µM EDTA and allowed to incubate along with the untreated control culture for the next 6 hrs at 30 °C with proper agitation. The total RNA was isolated by using MagSure All-RNA Isolation Kit, according to the manufacturer's instructions. The absorbance ratios of 260/280 and 260/230 were estimated using NanoDrop2000 to assess the concentration of RNA samples. Samples were also examined in 1 % agarose gel run at 70 V. The RNA was stored at -80 °C. Before RNA sequencing, QC was performed to check the quantity and integrity of RNA samples by using NanoDrop One and Qubit. The integrity of the RNA was checked by running on an Agilent Tapestation 4200 RNA HS Screentape to determine the RNA Integrity Number (RIN). For library preparation, RNA with >8 RIN values was processed. About 1 µg of RNA samples was depleted of Yeast rRNA using QIAseqFastSelect−rRNA yeast kit (Cat. no. 334215), according to the manufacturer's protocol. The NEBNext$^{(R)}$ Ultra II Directional RNA Library prep kit from Illumina (Cat. no. E7760L), was used to construct double-stranded cDNA libraries from the rRNA-depleted RNA. The cleaned libraries were quantitated on Qubit^{R}flurometer and appropriate dilutions were loaded on a High

sensitivity D1000 screen tape to determine the size range of fragments and the average library size (288-311 bp), followed by sequencing using Illumina NovaSeq.

Transcriptomics analysis: RNA-seq using Illumina generated raw data in FASTQ format. The raw data was analyzed using CLC genomics workbench 22.02 and quality control was assessed using the *QC plugin* of CLC to generate a minimum read length of 151 base pair. In order to filter and remove rRNA reads, *SortMeRNAv4.3.6* was used. Further quality trimming was performed to remove adaptors and low-quality ambiguous bases. Mapping of trimmed reads performed using *C. albicans* SC5314 reference genome (assembly ASM18296v3) downloaded from NCBI database. The uniquely mapped reads were selected as default followed by transcripts per million (TPM) as raw expression value. Gene expression (GE) track was used for profiling the differential gene expression, subsequently normalizing the trimmed mean of M values (TMM) using the edgeR method. In order to find the significant genes, two cut-off parameters; false discovery rate (FDR) cut-off ≤ 0.05 and log2 fold change (FC) cut-off ≥ 1 were applied to produce a differential gene expression (DEG) profile. Principal component analysis (PCA) was performed within R to project the high dimensional dataset onto a 2D or 3D plain based on the principal component specifying larger-sized variabilities. Data was represented and visualized through a heat map using the normalized log CPM values. The volcano plot was used to feature the gene of interest at the upper left- and right-hand corners, where log2 fold changes were plotted on the x-axis, and the -log10 p-values plotted on the y-axis. Pathway enrichment analysis was created based on gene ontology (GO), where GO terms were over-represented in a set of differentially expressed genes using ignore features with mean RPKM = 5, minimum absolute fold change = 1.5, and FDR p-value ≤ 0.05. KOBAS (KEGG Orthology Based Annotation System), a web server for gene/protein functional annotation (Annotation module) and functional set enrichment (Enrichment module) was used for pathway enrichment analysis. Gene interaction networks and protein-protein associations have been created using the STRING app. STRING software version 11.5 was used to undertake active parameters like text-mining, experiments, databases, co-expression, neighborhood, gene fusion, and co-occurrence for upregulated DEGs, while for downregulated DEGs, only the experimental parameter was considered. An interaction score of 0.7 (High confidence) was followed for all the STRING analyses.

Real-time and qRT-PCR: To validate the RNA seq data, cDNA was synthesized from 1000 ng RNA using a high-capacity cDNA synthesis kit (Thermo Fischer Scientific). The cDNA stock was diluted 30 times with nuclease-free water to prepare the working cDNA. For qRT, 5 µl of diluted cDNA along with 10 pmole of each from forward-reverse primers, and 2x SYBR Green reagent (Applied Biosystems™ PowerUp™ SYBR™ Green Master Mix, Thermo Fischer Scientific) was used. The amplification program consisted of the cyclic condition comprising 95 °C for 10 min on the holding stage, 95 °C for 15

sec, and 60 °C for 1 min on the PCR-cyclic stage, and 95 °C for 15 sec, 60 °C for 1 min and 95 °C for 15 sec on melting-curve stage, and 4 °C hold at one cycle (QuantStudio 3.0, Applied Biosystems). The mean C_t value of technical replicates from the standard curve was analyzed and plotted using The GraphPad Prism 8.0. Semi-quantitative RT-PCR assay was preceded with 10X PCR buffer, 10 mM dNTPs, 10 pmole concentration of each forward and reverse primers, and DNA Taq Polymerase. Samples were checked on agarose gel including *GAPDH* as a housekeeping gene. All the PCR primers and cyclic conditions are mentioned in **Suppl. Table S6**.

Transmission electron microscopy: The ultrathin section of *C. albicans* and CAET cells were examined and visualized by TEM. The *C. albicans* cells were subjected to aldehyde for pre-fixation and osmium tetraoxide for post-fixation followed by contrast staining using uranyl acetate as described before[37]. The hardened sample blocks were sectioned using Leica EM UC7 microtome and the samples on the copper grids were visualized under the JEM-2100Plus JEOL TEM imaging machine.

Measurement of cell wall contents by flow cytometry: The pre-culture of *C. albicans* was diluted to an OD_{600nm}=0.5 in 5 mL of YPD media. The culture was then treated with 250 µM EDTA and allowed to grow along with the untreated culture for 6 hrs at 30 °C and 200 rpm. For β (1, 3)-glucan estimation, aniline blue dye (Sigma, Cat. no. B8563) was added to 1 x 10^6 *C. albicans* cells/ml in a 1:1 ratio and incubated for 30 min at 30 °C. For chitin estimation, 1 x 10^6 cells/ml were treated with 2.5 µg concentration of Calcofluor White (Sigma, Cat. no. 910090) and incubated for 15 min at 25 ºC. Likewise, for the estimation of mannan, we used 10 µl of concanavalin A (1 mg/ml, Thermo Fischer Scientific, Cat. no. C860). The stained cells were centrifuged at 12,000 g for 1 min. The cell pellet was washed twice with 1 ml 1 X PBS and finally resuspended in 500 µl 1X PBS. The stained cells were then transferred to FACS tubes for acquisition. All the control and treated samples were acquired by BD LSR Fortessa Cell Analyzer using UV laser (350 nm) with a bandpass filter (450 nm/500 nm). The mean fluorescence intensity was obtained from the unstained and stained yeast cells and processed in flowJo software version 10.8.1. The assays were repeated twice with biological triplicates.

Polysome isolation and profiling: Polysome and its fractionation were carried out by using a protocol described before with slight modification[33]. Briefly, to isolate cell-free total ribosomes, *C. albicans* pre-culture was diluted to OD_{600nm} of 0.5 in YPD media to obtain 250 ml each in two flasks. While one of the cultures was treated with 250 µM EDTA, the other flask was kept untreated. The sub-cultures designated as *Ca* and CAET, respectively, were allowed to grow for ~ 6 hrs at 30 ºC and 200 rpm until the $OD_{600\ nm}$ becomes 0.8 – 1.0 (exponential phase). Cycloheximide (100 mg/ml) was added to the cultures 5 min before harvesting the cells. The cultures were kept for 15 min on ice and then centrifuged at 3000g at 4 ºC

for 5 min. The pellet was washed using 0.1 % autoclaved DEPC treated water and resuspended in 1.3 times total volume of the pellet weight using a lysis buffer (1 M Tris-Cl, 2 M KCl, 1 M $MgCl_2$, 10 % NP-40, 5 µl RNase Inhibitor, 20X Protease Inhibitor EDTA free, 200 µg/mL Cyclohexamide, DEPC H_2O). The re-suspended pellet was mixed thoroughly and 0.6 volume of acid-washed glass beads were added and homogenized in 5 cycles, each comprising 40 sec of vortexing at 6 m/s speed, with 2 min of ice incubation in between the cycles. The suspension was centrifuged at 3000g at 4 ºC for 10 min, the top lipid layer was carefully removed, and the supernatant was collected in a fresh tube. Subsequently, two additional rounds of centrifugation were carried out at 13K rpm at 4 ºC and each for 30 min. After each centrifugation, the supernatant was collected and transferred to a fresh Eppendorf tube. The absorbance of the supernatant was checked at 260 nm and the final OD for both the samples was adjusted to 20. For the preparation of a linear sucrose gradient, 10 % and 50 % sucrose were taken in polyallomer centrifuge tubes and the gradient was formed using a gradient maker (Gradient Master™ from BioComp). The cell free extracts (200 or 400 µl of OD=20) were added to the 10%-50% sucrose density gradients carefully, and ultracentrifuged using a SW41Ti rotor and Beckman Coulter Ultracentrifuge at 39K rpm for 2.5 h at 4ºC with the vacuum level of 200 microns. After the centrifugation, the fractions were collected carefully and the polysome profile was analyzed using the Density Gradient Fractionation System, which continuously scanned absorbance at 254 nm. The Density Gradient Fractionation System (BIOCOMP) was switched on approximately 1 hr before fractionation to ensure its readiness.

Macrophage Interaction: About 5 x 10^5 RAW 264.7 macrophage cells were seeded in a 12-well polystyrene plate containing DMEM supplemented with 10 % FBS. After 24 hrs of incubation, macrophages were washed with only DMEM and stained with a cell tracker deep red dye. After 45 min of incubation at 37 °C in a CO_2 incubator, the wells were washed with DMEM. The same number (5 x 10^5) freshly harvested *C. albicans* cells (*Ca* and CAET) were stained with CFSE for 1 hr. After straining, they were washed with 1X PBS and resuspended in DMEM media. The CFSE-stained fungal cells were added to each well having deep red-stained RAW cells and co-cultured at 37 °C. The control wells contained stained RAW cells only. At three different time points 1 hr, 2 hrs, and 3 hrs, the supernatant was discarded from the well to remove any non-phagocytosed fungal cells. The adhered cells were scrapped and transferred into the FACS tubes. After centrifugation, the cell pellet was resuspended in 500 µl of FACS buffer. The stained RAW cells were used for making a suitable gating strategy during fluorescence acquisition in a flow cytometer. The phagocytosis was determined by gating the cells and calculating the percentage of double-positive cells (CFSE-FITC & deep red- APC). For fungal clearance assay, a similar co-culture experiment was carried out by taking unstained macrophage cells but stained *C. albicans* cells. After completion of each time interval, the supernatant was aspirated to remove any free fungal cells and

1 ml of autoclaved warm distilled water (50 °C – 60 °C) was added to each well to release the phagocytosed *C. albicans*. The cells were scrapped and pooled down to the tube. Serial dilutions of cells were plated on an YPD plate treated with chloramphenicol. The plates were incubated at 30 °C for 48 hrs and CFU was determined. In macrophage killing assay, the wells comprising the macrophage-fungal cells co-culture were washed with 1 ml 1X PBS and stained with 200 ng/mL propidium iodide (MP-Biomedicals). Images were captured under a fluorescence microscope (EVOS imaging system; Thermo Fischer Scientific) after 2.5 hrs of incubation. The experiment was carried out in triplicates.

Systemic candidiasis in mice: 6-8 weeks BALB/c female mice were housed in a controlled and ventilated environment. To prepare the inoculum, the *C. albicans* pre-culture was diluted to an OD_{600nm}=0.5 (10^7 cells per mL) in YPD. About 10 ml of the diluted culture was grown further either untreated or treated with 250 μM EDTA for 6 hrs at 30 °C with shaking at 200 rpm. Both untreated and treated cells were harvested, re-suspended in 1X PBS, and cells were counted by using Neubauer chamber slide and online hemocytometer software (HemocyTap), and further confirmed by plating and CFU counting. After 7 days of acclimatization, depending upon the experiments, groups of mice (n=5/6) were challenged intravenously either with 5 x10^5 CFU of *C. albicans Ca* or CAET or the same volume (100 μl) of saline. The survivability of mice was monitored for 30 days. Based on the humane endpoints mice were euthanized. For kinetic analysis, mice were sacrificed on mentioned days of post infection. Various essential organs (brain, lungs, kidney, liver, and spleen) were excised for CFU analysis and PAS staining. For blood cell profiling and cytokine estimation, blood was drawn just before sacrificing. CFU analysis was carried out immediately after the dissection. The organs were thoroughly washed with PBS, homogenized in 1 mL of PBS, and appropriate serial dilutions were plated on YPD agar plates supplemented with 100 μg Chloramphenicol. The plates were incubated overnight to determine CFU/organ. The CFU/organ in Log_{10} scale and survival curves were plotted using GraphPad Prism 8 software. Mouse kidney paraffin sections were stained with PAS reagents as per the manufacturer's instructions and imaged under a Leica DM500 microscope.

Blood cells Profiling: Blood was obtained by slitting a small incision on the mice tail with the help of a scalpel and collected in tubes pre-filled with K_2-EDTA in a 1:10 ratio (Blood: K_2-EDTA). About 20 μl EDTA-anti coagulated blood samples were taken up in plastic capillaries (Kunstsoff-Kapillaren; 100120) and examined using an Exigo Blood Analyzer within 2 to 4 hrs of blood collection.

Cytokine and chemokine estimation: The BALB/c mice (n=3) from each category were intravenously injected with 5 x 10^5 CFU/ml *Ca* and CAET, and saline was taken as control. The mice were euthanized and the heart was punctured to obtain □500 μL of blood. The collected blood was stored at 4 ºC overnight

in an inclined position. Following the day, serum was collected carefully from each blood sample and transferred to a fresh tube. The collected serum was centrifuged at 5000 g for 20 min. The supernatant was collected and the level of the cytokines and chemokines was estimated by using Bio-Plex ProTM Mouse Cytokine standard 23-Plex (Bio-Rad, USA, Cat. no. 10014905). The kit was inbuilt and supplemented with 23 analytes. The graph was plotted using the GraphPad Prism 8 software.

Availability of data and materials

Raw RNA seq reads were deposited in a public database and can be retrieved by using the accession number PRJNA1010013. Rest of the data has been provided in the paper.

Competing interests

NA and SB are listed as inventors in a related patent application. The remaining authors declare no competing interests.

Funding

This work was supported by the intramural core grant from ILS and extramural research funds from DBT, India (BT/PR32817/MED/29/1495/2020).

Authors' contributions

NA conceptualized, designed, supervised, and analyzed the study; SB, SRS, and AD generated materials, conducted experiments, analyzed the data, and prepared an initial draft of the manuscript. NA, SB, SRS, and AD wrote the final draft. NA obtained the funding. All the authors reviewed the results and approved the final version of the manuscript.

Acknowledgements: We thank Mr. Sitendra Prasad Panda and Mr. Paritosh Nath for their technical assistance. Dr. Sarita Jena, Mr. Biswajit Patro, and Mr. Subrat Kumar Naik for technical assistance and nurturing of the animals were highly appreciated. Ms. Tanvi Sinha and Dr. Amaresh Panda for helping us during polysome isolation and profiling. We thank our other laboratory colleagues for their thoughtful discussion. SB and SRS are grateful for SERB/UGC-Senior Research Fellowships and AD is thankful for the DBT-RA fellowship. ILS animal house, TEM Imaging, and FACS facilities are highly acknowledged.

References

1 Brown, G. D. *et al.* Hidden killers: human fungal infections. *Sci Transl Med* **4**, 165rv113, doi:10.1126/scitranslmed.3004404 (2012).

2 Peroumal, D., Sahu, S. R., Kumari, P., Utkalaja, B. G. & Acharya, N. Commensal Fungus Candida albicans Maintains a Long-Term Mutualistic Relationship with the Host To Modulate Gut Microbiota and Metabolism. *Microbiol Spectr* **10**, e0246222, doi:10.1128/spectrum.02462-22 (2022).

3 Ford, C. B. *et al.* The evolution of drug resistance in clinical isolates of Candida albicans. *eLife* **4**, e00662, doi:10.7554/eLife.00662 (2015).

4 Lee, Y., Puumala, E., Robbins, N. & Cowen, L. E. Antifungal Drug Resistance: Molecular Mechanisms in Candida albicans and Beyond. *Chem Rev* **121**, 3390-3411, doi:10.1021/acs.chemrev.0c00199 (2021).

5 Rudkin, F. M. *et al.* Single human B cell-derived monoclonal anti-Candida antibodies enhance phagocytosis and protect against disseminated candidiasis. *Nature communications* **9**, 5288, doi:10.1038/s41467-018-07738-1 (2018).

6 Sahu, S. R. *et al.* Vaccines against candidiasis: Status, challenges and emerging opportunity. *Front Cell Infect Microbiol* **12**, 1002406, doi:10.3389/fcimb.2022.1002406 (2022).

7 Edwards, J. E., Jr. *et al.* A Fungal Immunotherapeutic Vaccine (NDV-3A) for Treatment of Recurrent Vulvovaginal Candidiasis-A Phase 2 Randomized, Double-Blind, Placebo-Controlled Trial. *Clinical infectious diseases : an official publication of the Infectious Diseases Society of America* **66**, 1928-1936, doi:10.1093/cid/ciy185 (2018).

8 De Bernardis, F. *et al.* A virosomal vaccine against candidal vaginitis: immunogenicity, efficacy and safety profile in animal models. *Vaccine* **30**, 4490-4498, doi:10.1016/j.vaccine.2012.04.069 (2012).

9 Netea, M. G., Joosten, L. A., van der Meer, J. W., Kullberg, B. J. & van de Veerdonk, F. L. Immune defence against Candida fungal infections. *Nat Rev Immunol* **15**, 630-642, doi:10.1038/nri3897 (2015).

10 Romani, L. Immunity to fungal infections. *Nat Rev Immunol* **4**, 1-23, doi:10.1038/nri1255 (2004).

11 Cardenas-Freytag, L. *et al.* Partial protection against experimental vaginal candidiasis after mucosal vaccination with heat-killed Candida albicans and the mucosal adjuvant LT(R192G). *Medical mycology* **40**, 291-299 (2002).

12 Liu, M. *et al.* Saccharomyces as a vaccine against systemic candidiasis. *Immunol Invest* **41**, 847-855, doi:10.3109/08820139.2012.692418 (2012).

13 Saville, S. P., Lazzell, A. L., Chaturvedi, A. K., Monteagudo, C. & Lopez-Ribot, J. L. Efficacy of a genetically engineered Candida albicans tet-NRG1 strain as an experimental live attenuated vaccine against hematogenously disseminated candidiasis. *Clinical and vaccine immunology : CVI* **16**, 430-432, doi:10.1128/CVI.00480-08 (2009).

14 Hood, M. I. & Skaar, E. P. Nutritional immunity: transition metals at the pathogen-host interface. *Nature reviews. Microbiology* **10**, 525-537, doi:10.1038/nrmicro2836 (2012).

15 Gerwien, F., Skrahina, V., Kasper, L., Hube, B. & Brunke, S. Metals in fungal virulence. *FEMS Microbiol Rev* **42**, doi:10.1093/femsre/fux050 (2018).

16 Crawford, A. & Wilson, D. Essential metals at the host-pathogen interface: nutritional immunity and micronutrient assimilation by human fungal pathogens. *FEMS yeast research* **15**, doi:10.1093/femsyr/fov071 (2015).

17 Almeida, R. S. *et al.* the hyphal-associated adhesin and invasin Als3 of Candida albicans mediates iron acquisition from host ferritin. *PLoS pathogens* **4**, e1000217, doi:10.1371/journal.ppat.1000217 (2008).

18 Citiulo, F. *et al.* Candida albicans scavenges host zinc via Pra1 during endothelial invasion. *PLoS pathogens* **8**, e1002777, doi:10.1371/journal.ppat.1002777 (2012).

19 Bates, S. *et al.* Candida albicans Pmr1p, a secretory pathway P-type Ca2+/Mn2+-ATPase, is required for glycosylation and virulence. *The Journal of biological chemistry* **280**, 23408-23415, doi:10.1074/jbc.M502162200 (2005).

20 Bose, S., Singh, D. V., Adhya, T. K. & Acharya, N. Escherichia coli, but Not Staphylococcus aureus, Functions as a Chelating Agent That Exhibits Antifungal Activity against the Pathogenic Yeast Candida albicans. *J Fungi (Basel)* **9**, doi:10.3390/jof9030286 (2023).
21 Polvi, E. J. *et al.* Metal Chelation as a Powerful Strategy to Probe Cellular Circuitry Governing Fungal Drug Resistance and Morphogenesis. *PLoS genetics* **12**, e1006350, doi:10.1371/journal.pgen.1006350 (2016).
22 Cho, Y. E. *et al.* Cellular Zn depletion by metal ion chelators (TPEN, DTPA and chelex resin) and its application to osteoblastic MC3T3-E1 cells. *Nutrition research and practice* **1**, 29-35, doi:10.4162/nrp.2007.1.1.29 (2007).
23 Niewerth, M. *et al.* Ciclopirox olamine treatment affects the expression pattern of Candida albicans genes encoding virulence factors, iron metabolism proteins, and drug resistance factors. *Antimicrobial agents and chemotherapy* **47**, 1805-1817 (2003).
24 Bleackley, M. R. *et al.* Bovine pancreatic trypsin inhibitor is a new antifungal peptide that inhibits cellular magnesium uptake. *Molecular microbiology* **92**, 1188-1197, doi:10.1111/mmi.12621 (2014).
25 Wilson, D., Citiulo, F. & Hube, B. Zinc exploitation by pathogenic fungi. *PLoS pathogens* **8**, e1003034, doi:10.1371/journal.ppat.1003034 (2012).
26 Lan, C. Y. *et al.* Regulatory networks affected by iron availability in Candida albicans. *Molecular microbiology* **53**, 1451-1469, doi:10.1111/j.1365-2958.2004.04214.x (2004).
27 Kuznets, G. *et al.* A relay network of extracellular heme-binding proteins drives C. albicans iron acquisition from hemoglobin. *PLoS pathogens* **10**, e1004407, doi:10.1371/journal.ppat.1004407 (2014).
28 Zheng, X., Wang, Y. & Wang, Y. Hgc1, a novel hypha-specific G1 cyclin-related protein regulates Candida albicans hyphal morphogenesis. *The EMBO journal* **23**, 1845-1856, doi:10.1038/sj.emboj.7600195 (2004).
29 Ducker, G. S. & Rabinowitz, J. D. One-Carbon Metabolism in Health and Disease. *Cell Metab* **25**, 27-42, doi:10.1016/j.cmet.2016.08.009 (2017).
30 Akanuma, G. Diverse relationships between metal ions and the ribosome. *Bioscience, biotechnology, and biochemistry* **85**, 1582-1593, doi:10.1093/bbb/zbab070 (2021).
31 Kapteyn, J. C. *et al.* The cell wall architecture of Candida albicans wild-type cells and cell wall-defective mutants. *Molecular microbiology* **35**, 601-611 (2000).
32 Klein, D. J., Moore, P. B. & Steitz, T. A. The contribution of metal ions to the structural stability of the large ribosomal subunit. *Rna* **10**, 1366-1379, doi:10.1261/rna.7390804 (2004).
33 Pospisek, M. & Valasek, L. Polysome profile analysis--yeast. *Methods in enzymology* **530**, 173-181, doi:10.1016/B978-0-12-420037-1.00009-9 (2013).
34 Netea, M. G., Brown, G. D., Kullberg, B. J. & Gow, N. A. An integrated model of the recognition of Candida albicans by the innate immune system. *Nature reviews. Microbiology* **6**, 67-78, doi:10.1038/nrmicro1815 (2008).
35 Kumari, P., Sahu, S. R., Utkalaja, B. G., Dutta, A. & Acharya, N. RAD51-WSS1-dependent genetic pathways are essential for DNA-protein crosslink repair and pathogenesis in Candida albicans. *The Journal of biological chemistry* **299**, 104728, doi:10.1016/j.jbc.2023.104728 (2023).
36 Peroumal, D. *et al.* Virulence and pathogenicity of a Candida albicans mutant with reduced filamentation. *Cellular microbiology* **21**, e13103, doi:10.1111/cmi.13103 (2019).
37 Patel, S. K., Sahu, S. R., Utkalaja, B. G., Bose, S. & Acharya, N. Pol32, an accessory subunit of DNA polymerase delta, plays an essential role in genome stability and pathogenesis of Candida albicans. *Gut Microbes* **15**, 2163840, doi:10.1080/19490976.2022.2163840 (2023).
38 Spellberg, B., Ibrahim, A. S., Edwards, J. E., Jr. & Filler, S. G. Mice with disseminated candidiasis die of progressive sepsis. *The Journal of infectious diseases* **192**, 336-343, doi:10.1086/430952 (2005).

39 MacCallum, D. M., Castillo, L., Brown, A. J., Gow, N. A. & Odds, F. C. Early-expressed chemokines predict kidney immunopathology in experimental disseminated Candida albicans infections. *PloS one* **4**, e6420, doi:10.1371/journal.pone.0006420 (2009).

40 Gil, M. L., Casanova, M. & Martinez, J. P. Changes in the cell wall glycoprotein composition of Candida albicans associated to the inhibition of germ tube formation by EDTA. *Arch Microbiol* **161**, 489-494, doi:10.1007/BF00307769 (1994).

41 Sen, B. H., Akdeniz, B. G. & Denizci, A. A. The effect of ethylenediamine-tetraacetic acid on Candida albicans. *Oral surgery, oral medicine, oral pathology, oral radiology, and endodontics* **90**, 651-655, doi:10.1067/moe.2000.109640 (2000).

42 Pugh, D. & Cawson, R. A. Calcium, sequestering agents and nystatin--interactions on cell wall morphology and fungistasis of Candida albicans. *Sabouraudia* **18**, 157-159, doi:10.1080/00362178085380251 (1980).

43 Casalinuovo, I. A., Sorge, R., Bonelli, G. & Di Francesco, P. Evaluation of the antifungal effect of EDTA, a metal chelator agent, on Candida albicans biofilm. *European review for medical and pharmacological sciences* **21**, 1413-1420 (2017).

44 de Oliveira, H. C. *et al.* Identification of Off-Patent Compounds That Present Antifungal Activity Against the Emerging Fungal Pathogen Candida auris. *Front Cell Infect Microbiol* **9**, 83, doi:10.3389/fcimb.2019.00083 (2019).

45 Laskaris, P. *et al.* Administration of Zinc Chelators Improves Survival of Mice Infected with Aspergillus fumigatus both in Monotherapy and in Combination with Caspofungin. *Antimicrobial agents and chemotherapy* **60**, 5631-5639, doi:10.1128/AAC.00324-16 (2016).

46 Besold, A. N. *et al.* Role of Calprotectin in Withholding Zinc and Copper from Candida albicans. *Infection and immunity* **86**, doi:10.1128/IAI.00779-17 (2018).

47 Hunsaker, E. W. & Franz, K. J. Candida albicans reprioritizes metal handling during fluconazole stress. *Metallomics : integrated biometal science* **11**, 2020-2032, doi:10.1039/c9mt00228f (2019).

48 Hans, S., Fatima, Z. & Hameed, S. Magnesium deprivation affects cellular circuitry involved in drug resistance and virulence in Candida albicans. *J Glob Antimicrob Resist* **17**, 263-275, doi:10.1016/j.jgar.2019.01.011 (2019).

49 Zipfel, P. F., Skerka, C., Kupka, D. & Luo, S. Immune escape of the human facultative pathogenic yeast Candida albicans: the many faces of the Candida Pra1 protein. *Int J Med Microbiol* **301**, 423-430, doi:10.1016/j.ijmm.2011.04.010 (2011).

50 MacCallum, D. M. *et al.* Property differences among the four major Candida albicans strain clades. *Eukaryotic cell* **8**, 373-387, doi:10.1128/EC.00387-08 (2009).

51 Richard, M. L. & Plaine, A. Comprehensive analysis of glycosylphosphatidylinositol-anchored proteins in Candida albicans. *Eukaryotic cell* **6**, 119-133, doi:10.1128/EC.00297-06 (2007).

52 Gelis, S. *et al.* Pga13 in Candida albicans is localized in the cell wall and influences cell surface properties, morphogenesis and virulence. *Fungal genetics and biology : FG & B* **49**, 322-331, doi:10.1016/j.fgb.2012.01.010 (2012).

53 Plaine, A. *et al.* Functional analysis of Candida albicans GPI-anchored proteins: roles in cell wall integrity and caspofungin sensitivity. *Fungal genetics and biology : FG & B* **45**, 1404-1414, doi:10.1016/j.fgb.2008.08.003 (2008).

54 Sanglard, D., Hube, B., Monod, M., Odds, F. C. & Gow, N. A. A triple deletion of the secreted aspartyl proteinase genes SAP4, SAP5, and SAP6 of Candida albicans causes attenuated virulence. *Infection and immunity* **65**, 3539-3546, doi:10.1128/iai.65.9.3539-3546.1997 (1997).

55 Tsuchimori, N. *et al.* Reduced virulence of HWP1-deficient mutants of Candida albicans and their interactions with host cells. *Infection and immunity* **68**, 1997-2002, doi:10.1128/IAI.68.4.1997-2002.2000 (2000).

56 Daniels, K. J., Lockhart, S. R., Staab, J. F., Sundstrom, P. & Soll, D. R. The adhesin Hwp1 and the first daughter cell localize to the a/a portion of the conjugation bridge during Candida albicans mating. *Molecular biology of the cell* **14**, 4920-4930, doi:10.1091/mbc.e03-04-0264 (2003).

57 Banerjee, M. *et al.* UME6, a novel filament-specific regulator of Candida albicans hyphal extension and virulence. *Molecular biology of the cell* **19**, 1354-1365, doi:10.1091/mbc.e07-11-1110 (2008).
58 Lin, C. H. *et al.* Genetic control of conventional and pheromone-stimulated biofilm formation in Candida albicans. *PLoS pathogens* **9**, e1003305, doi:10.1371/journal.ppat.1003305 (2013).
59 Balish, E., Wagner, R. D., Vazquez-Torres, A., Pierson, C. & Warner, T. Candidiasis in interferon-gamma knockout (IFN-gamma-/-) mice. *The Journal of infectious diseases* **178**, 478-487, doi:10.1086/515645 (1998).
60 Cenci, E. *et al.* Interleukin-4 causes susceptibility to invasive pulmonary aspergillosis through suppression of protective type I responses. *The Journal of infectious diseases* **180**, 1957-1968, doi:10.1086/315142 (1999).
61 Haraguchi, N. *et al.* Impairment of host defense against disseminated candidiasis in mice overexpressing GATA-3. *Infection and immunity* **78**, 2302-2311, doi:10.1128/IAI.01398-09 (2010).
62 Huang, W., Na, L., Fidel, P. L. & Schwarzenberger, P. Requirement of interleukin-17A for systemic anti-Candida albicans host defense in mice. *The Journal of infectious diseases* **190**, 624-631, doi:10.1086/422329 (2004).
63 Traynor, T. R. & Huffnagle, G. B. Role of chemokines in fungal infections. *Medical mycology* **39**, 41-50, doi:10.1080/mmy.39.1.41.50 (2001).
64 Drago, L., Bortolin, M., Vassena, C., Taschieri, S. & Del Fabbro, M. Antimicrobial activity of pure platelet-rich plasma against microorganisms isolated from oral cavity. *BMC microbiology* **13**, 47, doi:10.1186/1471-2180-13-47 (2013).

Figure Legends:

Figure 1. Effect of metal chelators on the growth and biofilm of *C. albicans.* (A) *C. albicans* cells were cultured in YPD media at 30 °C for 24 hrs without (cyan blue) and with the indicated concentration of EDTA (purple), $MgSO_4$ (Green), $ZnCl_2$ (Grey), $FeCl_2$ (Brown), and $MnCl_2$ (Black), EDTA+$MgSO_4$ (Lime green), EDTA+$MgSO_4$@6 hr (dark blue), EDTA+$ZnCl_2$ (Maroon), EDTA+$FeCl_2$ (Orange), and EDTA+$MnCl_2$ (Pink). Optimal absorbance was measured at 600 nm in different intervals of incubation. **(B)** The cultures from the above mentioned experiment was diluted and plated on YPD plate. Colonies were counted and plotted to determine the CFU efficiency. **(C)** Pre-formed *C. albicans* biofilm was treated with EDTA and divalent metals as mentioned. Their effect on biofilm was observed post-24 h treatment by crystal violet staining and estimating at 570 nm. **(D)** Effect of EDTA and divalent metals on *C. albicans* biofilm was again observed by acridine orange staining and visualization under a 40X magnification using a CLSM. Similarly, the effect of other metal chelators like DTPA (Lime green), Aprotinin (blue), TPEN (orange) and CE (grey) on the growth (**E**), CFU (**F**), and biofilm formation of *C. albicans* analyzed by crystal violet staining (**G**) and CLSM (**H**). Mean values from three independent experiments considered and error bar represents SEM. *p* values *< 0.05, **<0.01 and ****< 0.0001 were significant as determine by one-way ANOVA.

Figure 2. Transcriptomics analyses *C. albicans* cells upon EDTA treatment. (A) A Volcano plot depicting differentially expressed genes (DEGs) in CAET cells. The red dots indicate upregulated genes (411) and blue dots indicates the downregulated genes (388). **(B)** Heat map showing relative abundance of top 25 significantly upregulated and downregulated genes in *Ca* and CAET. RNA sequencing was carried out in triplicates. Red colour indicates upregulation and blue indicates downregulation as denoted by the Z score. **(C)** Double donut chart indicates top 100 significantly upregulated genes categorized into four main groups i.e., metal transporters (light green), cell wall- and membrane-associated genes other than metal transporters (blue), others (includes drugs resistance-associated, morphology-associated, biosynthetic and catalytic processes; represented in grey), and uncharacterized genes (cream). Inner donut depicts the number of DEGs from the above categories associated with virulence and pathogenesis in *C. albicans* as reported by published literatures. **(D)** Double donut chart depicting top 100 significant downregulated gene categorized as metabolic pathways (green), cell-wall associated (blue), ribosomal (grey), others (includes morphology-associated, resistance-associated; represented in yellow), and uncharacterized (cream). Outer circle represents the total number of genes in each category and inner circle indicates the virulence-related genes out of the total number of genes in that specific category. **(E)** Gene ontology enrichment analysis for 411 upregulated DEGs. **(F)** Gene ontology enrichment analysis for 388 downregulated DEGs were plotted. Both in (E) and (F), *x*-axis represents the number of DEGs and *y*-axis represents various processes like BP (biological processes), MF (molecular functions), and CC (cellular components) indicated in maroon, blue, and grey colors, respectively. (**G**) STRING analyses showing relationship between DEGs. Interaction amongst 15 connected out of 31 upregulated DEGs involved in metal transport and homeostasis is shown. (**H**) STRING analysis shows 9 connected out of 33 upregulated DEGs involved in pathogenesis. **(I**) Among the down-regulated DEGs, 70 connected out of 74 DEGs belonging to cytosolic ribosomal genes as determined by STRING. (J) 38 connected out of 56 DEGs belonging to mitochondrial ribosomal components were connected by as determined STRING.

Figure 3. Effect of EDTA on the cell wall and polysome of *C. albicans*. (A) Showing TEM images of ultrathin sections of untreated (*Ca)* and EDTA-treated (CAET) *C. albicans* at different resolution. Samples visualized at 14000 X magnification, arrow indicates the marked cell, and box indicates the focus area where thickness was measured. Scale bar = 2 µm for intact cells (i); scale bar = 1 µm for a single cell (ii); scale bar=500 nm for zoomed in image of an individual cell wall (iii). (**B**) *C. albicans* cells were stained with Con A and analyzed by flow cytometry (i) and mean fluorescence intensity was measured to estimate the mannan level (ii). **(C)** *C. albicans* cells were stained with aniline blue and analyzed by flow cytometry (i) and mean fluorescence intensity was measured to estimate the β-glucan level (ii). **(D)** *C. albicans* cells were stained with calcofluor white and analyzed by flow cytometry (i) and

mean fluorescence intensity was measured to estimate the chitin level (ii). Mean average of three independent biological replicates with error bars is shown. *p* values *< 0.05 and ***< 0.001 as determined by unpaired t-test. **(E)** Cell-free total ribosomes were isolated by taking two different concentrations (pellet size of 200 µL and 400 µL) of *C. albicans* cells (*Ca* and CAET) and fractionated using sucrose gradient centrifugation. Fractions were analysed and plotted. The position and transition of ribosome subunits, monosome and polysome peaks were as shown.

Figure 4. *C. albicans*-Macrophage interaction. (A) Deep red-stained RAW 264.7 murine macrophage cells were co-cultured with *C. albicans* (*Ca* and CAET) in 1:1 ratio. After each time point (1 hr, 2 hrs and 3 hrs) cells were pooled down and double positive cells (CFSE-FITC channel and deep red-APC channel; Q2, P3) were analysed by flow cytometry **(i)**. Mean florescence intensity of three independent biological replicates were plotted using the GraphPad Prism software **(ii)**. **(B)** From a similar co-culture experiment**,** *C. albicans* cells (*Ca* and CAET) were retrieved from macrophage cells and plated on YPD/Chloramphenicol plate by taking appropriate dilutions. The plates were incubated at 30 ºC for 48 hrs. The plates were imaged (**i**) and colony-forming unit (CFU) was determined **(ii)**. **(C)** A similar co-culture of macrophage and *C. albicans* (*Ca* and CAET) were carried out for 2.5 hrs and the dying macrophages were observed by propidium iodide staining (Red dots). Images were captured with fluorescence microscope (EVOS imaging system; Thermo Fisher Scientific) at 20X and 40X magnifications **(i)** and the population of dead macrophages were determined **(ii)**. *p* values *< 0.05, **< 0.01, and ***< 0.01 as determined by two-way ANOVA.

Figure 5. Systemic candidiasis development and progression in *C. albicans* challenged mice. (A) Mice (n=6/category) were injected intravenously with 5 x 10^5 *C. albicans* cells (*Ca*: cyan blue and CAET: purple) and saline as control (grey) and their survivability was monitored for 30 days. In a similar set of experiment, mice (n=6/category) were first immunized with CAET (represented in brown) or sham vaccinated with saline (represented in orange), and after 30 days, they were further re-challenged with *C. albicans*. Their survivability was monitored for another 30 days and a survival curve was plotted. The number of sacrificed mice were mentioned on the particular days in the survival plot. 1° and 2° suggest primary and secondary challenges, respectively. Statistical significance of the survival curve was determined using Mantel-Cox test. *p* values were as mentioned, otherwise they were non-significant. Y-axis was represented in Log rank scale. **(B)** Fungal load in the kidney, liver, and spleen of sacrificed mice in Log_{10} scale was determined by CFU analyses. No statistical significant difference was observed between these groups. **(C)** PAS-staining for one of the kidneys carried out to visualize the fungal burden in the cortex and medulla regions under 40X magnification. **(D)** To check the disease progression, a kinetic experiment was planned as indicated in the schematic diagram. A group of mice were injected

intravenously with 5 x 10^5 *C. albicans* cells (*Ca*: cyan blue, CAET: purple, and 1° CAET 2°*Ca*: brown) and saline controls (grey and green) at 0 day, and five mice from each group were sacrificed on each day mentioned (3rd, 7th, 10th, 20th, and 30th day). Approximately 20 µl blood was drawn from the lateral tail vein of the mice prior to sacrifice. **(E)** Fungal load in the brain, liver, kidney, and spleen in Log_{10} scale was determined by CFU analyses. **(F)** Blood parameters such as WBC, Granulocytes, Platelets, and Monocytes levels were analyzed on the above-mentioned days and graphs were plotted using the GraphPad Prism software. The statistical analyses between saline and fungal infected mice groups of same day sacrificed were carried out. *p* values **<0.01, **<0.01, ***<0.00, and ****< 0.0001 as determined by two-way ANOVA.

Figure 6. Cytokine and chemokine estimation in infected mice. The mice (n=3/category) were inoculated with *Ca* or CAET or saline and sacrificed on various days as indicated and cytokine and chemokine levels in the blood serum were quantified by using Bio-plex Pro™ cytokine multiplex kit. **(A)** A panel of Th-1 cytokines, i.e., IL-1α, IL-1β, IL2, IL-10, IL-12(p40), IL-12(p70), IFN-γ, TNF-α, and GM-CSF, **(B)** Th-2/Th-17 cytokines, i.e., IL-3, IL-4, IL-5, IL-6, IL-9, IL-13, and IL-17, and **(C)** Chemokines i.e., RANTES, MCP-1, MIP-1α, MIP-1β, KC, and EOTAXIN. The statistical analyses between saline and fungal infected mice groups of same day sacrificed were carried out. *p* values **<0.01, **<0.01, ***<0.00, and ****< 0.0001 as determined by two-way ANOVA.

Figure 7. Model depicting the attributes of CAET cells. EDTA alters the cell wall thickness by altering its composition. Metal transporters and several cell wall and membrane associated genes get upregulated. To mitigate the essential metal scarcity, genes involved in ribosome biogenesis and one-carbon metabolism were down-regulated. CAET cells get phagocytosed efficiently and eliminated faster by macrophages. CAET infected mice survived and induced robust host immune responses to protect the lethal challenge. Thus, CAET is a potential live whole-cell vaccine candidate.

Table 1: A brief summary of RNA sequencing reads obtained from Illumina Novaseq

Sample Name (Sequencing ID	Read Length (bp)	Total raw reads	Reads after rRNA removal	Avergae Length after trim	Read after trimming	% known mRNA	% Unknown mRNA
Wild type (MT523)	151x2	21,937,416	19,222,356 (87.62%)	143.22	19,221,728	98.06	1.94
Wild type (MT524)	151x2	20,794,992	18,475,070 (88.84%)	141.71	18,474,428	98.32	1.68
Wild type (MT525)	151x2	20,564,218	17,699,794 (86.07%)	140.89	17,699,180	98.3	1.7
CAET (MT526)	151x2	22,376,466	20,284,442 (90.65%)	140.79	20,283,776	98.15	1.85
CAET (MT527)	151x2	21,412,804	20,073,926 (97.49%)	142.14	20,073,230	98.72	1.28
CAET (MT528)	151x2	20,435,938	19,391,726 (94.89%)	142.25	19,391,142	98.85	1.15

Table 2: List of top 100 upregulated genes in EDTA treated *C. albicans* cell (CAET)

Metal Transporters				
No. of DEGs	**Name of DEGs (13)**	**Fold Change**	**FDR p-value**	**Function**
1	ZRT1	5644.9942	5.20999E-82	Zinc ion transporter; Hyphal inducer
2	PRA1	1829.3467	1.3833E-282	Zinc sequester; pH regulated antigen
3	CFL5	151.1291	4.16014E-13	Ferric reductase
4	CFL2	94.2481	1.5889E-282	Ferric reductase; Virulence
5	PHO87	90.3067	1.0754E-176	Phosphate transporter; Virulence
6	ZRT2	68.1720	2.5856E-297	Zinc uptake; Biofilm inducer
7	CSA2	26.6647	0.000886698	Hyphal inducer; Heme utilization protein; Biofilm inducer
8	CSR1	23.2254	2.0725E-222	zinc homeostasis, Filamentation inducer;
9	CSA1	22.5038	3.4486E-166	Hyphal inducer; Iron homeostasis; Biofilm inducer;
10	HAP3	18.4511	5.412E-13	Iron homeostasis;
11	CFL4	8.4663	3.22997E-11	Uptake of iron metal ion
12	FRE9	7.5052	1.41623E-45	Ion transport, Ferric reductase
13	ARH2	5.7589	1.18159E-60	Involved in heme biosynthesis
Cell-wall and -membrane associated				
	Name of the DEGs (15)	**Fold Change**	**FDR p-value**	**Function**
1	SCW4	28.9947	0.000794714	Glucanase activity
2	PGA13	26.3347	8.3797E-163	Cell wall integrity; Morphogenesis, Virulence
3	PGA31	22.0969	1.25365E-18	Cell wall integrity
4	CHT4	20.7121	4.5927E-126	Chitin synthesis and degradation
5	RIM9	12.4158	4.4708E-121	Promote growth under alkaline condition
6	ALS4	10.0218	1.4683E-110	Enhance cell surface adhesion
7	CSH1	9.5387	1.2788E-107	Maintain cell integrity; Virulence
8	MRV8	8.7526	0.007934383	Biofilm inducer; Caspofungin tolerance
9	HGT5	7.5433	2.42539E-86	Glucose transporter
10	CDA2	7.2664	1.39323E-07	Chitin deacetylase
11	PRN4	6.2037	5.00644E-35	Protein with similarity to pirins
12	GLX3	5.9890	3.73497E-61	Binds human IgE; Induce biofilm
13	PGA7	5.6247	2.14119E-46	GPI-linked hyphal surface antigen; Induce spider biofilm
14	RBT5	5.5414	7.36268E-45	GPI-linked cell wall protein; utilize haemin and haemoglobin; biofilm induced

15	JEN1	5.1930	4.63735E-06	Localized on plasma membrane and induced by lactic acid
Others				
	Name of the DEGs (15)	**Fold Change**	**FDR p-value**	**Function**
1	LAP3	20.7648	6.7063E-221	Aminopeptidase; Bleomycin resistance
2	IFD6	18.4736	2.2359E-181	Azole resistance; Biofilm-inducer
3	ATO1	13.3199	6.23932E-08	pH neutralizer in macrophage phagolysosome
4	NOP6	10.5223	3.90346E-07	Ribosome biosynthesis
5	RAS2	10.2667	8.69395E-36	Filamentous growth enhancer; cAMP pathway regulator
6	HST6	8.6960	6.13855E-09	Transport lipid; antifungal drugs resistance; Encode ABC transporters
7	STE23	8.3030	3.41151E-92	Involved in processing of mating pheromones
8	FGR46	7.4482	1.72544E-07	Filamentous Growth Regulator
9	POL93	7.0291	1.77132E-69	Encode reverse transcriptase, protease and integrase; Induce biofilm
10	HPD1	5.9926	6.53346E-22	Involved in degradation of toxic propionyl-CoA; Induce spider biofilm
11	AOX2	5.6936	7.2209E-114	Induce biofilm formation
12	SOU2	5.5746	0.006421918	L-sorbose utilization; biofilm induced
13	GPD1	5.4805	2.01281E-74	Involved in glycerol biosynthesis
14	CAG1	5.3023	2.20049E-05	Role in mating pheromone response
15	FDH1	5.2775	2.01281E-74	oxidization of formate to CO2
Uncharacterized				
	Name (57 DEGs)	**Fold Change**	**FDR p-value**	**Function**
1	CAALFM_C200860CA	1600.2301	4.4708E-121	Uncharacterized
2	CAALFM_C401340WA	583.6099	0.000537249	Uncharacterized
3	CAALFM_CR08740WA	64.8421	0.035751787	Uncharacterized
4	CAALFM_CR02340WA	53.5609	3.38443E-05	Uncharacterized
5	CAALFM_CR07740WA	42.2094	1.62356E-12	Uncharacterized
6	CAALFM_C602100WA	32.1762	0.000435707	Uncharacterized
7	CAALFM_C104010CA	21.9880	4.8225E-124	Uncharacterized
8	CAALFM_C604230WA	19.1498	1.67518E-34	Uncharacterized
9	CAALFM_C110050WA	18.1320	0.000124176	Uncharacterized
10	CAALFM_CR06510WA	17.4047	6.21185E-37	Uncharacterized
11	CAALFM_CR06500CA	13.6055	2.25687E-88	Uncharacterized

12	CAALFM_CR08310CA	10.6593	4.21036E-20	Uncharacterized
13	CAALFM_CR06570CA	10.6284	6.6067E-77	Uncharacterized
14	CAALFM_C204430WA	9.9253	0.003875235	Uncharacterized
15	CAALFM_C303570CA	9.6111	5.27224E-07	Uncharacterized
16	CAALFM_C306040WA	9.4663	1.09545E-56	Uncharacterized
17	CAALFM_C106860WA	9.4073	0.000100814	Uncharacterized
18	CAALFM_C602480WA	9.3877	1.58803E-89	Uncharacterized
19	CAALFM_C302790WA	9.1272	2.43382E-06	Uncharacterized
20	CAALFM_C503430WA	8.6904	0.000101716	Uncharacterized
21	CAALFM_C402930WA	8.6463	2.18312E-11	Uncharacterized
22	CAALFM_C403340CA	8.6294	0.000183681	Uncharacterized
23	CAALFM_C701010WA	8.4791	3.30179E-61	Uncharacterized
24	CAALFM_C202580WA	8.4163	0.001492629	Uncharacterized
25	CAALFM_C405830WA	8.3518	3.67121E-05	Uncharacterized
26	CAALFM_C304210WA	8.1065	3.03712E-07	Uncharacterized
27	CAALFM_C406150CA	7.9704	0.014291503	Uncharacterized
28	CAALFM_C303370CA	7.9704	1.1929E-135	Uncharacterized
29	CAALFM_C204450WA	7.8462	6.43154E-11	Uncharacterized
30	CAALFM_C202180WA (ZRT3)	7.7272	3.31888E-71	Uncharacterized
31	CAALFM_C100270WA	7.1398	4.2578E-73	Uncharacterized
32	CAALFM_C401860CA	7.0743	1.14226E-09	Uncharacterized
32	CAALFM_C302360CA	6.7969	5.99145E-37	Uncharacterized
34	CAALFM_C600980CA	6.6896	7.44423E-52	Uncharacterized
35	CAALFM_CR06310WA	6.6535	0.00233344	Uncharacterized
36	CAALFM_C202750CA	6.5793	0.000307212	Uncharacterized
37	CAALFM_C200760CA	6.4769	1.48506E-85	Uncharacterized
38	CAALFM_C104690CA	6.2900	1.03644E-05	Uncharacterized
39	CAALFM_C304350CA	6.2289	1.2123E-25	Uncharacterized
40	CAALFM_C207620WA	6.1661	6.18529E-06	Uncharacterized
41	CAALFM_CR01910CA	6.0167	0.000328533	Uncharacterized
42	CAALFM_C702280WA	6.0140	0.037653707	Uncharacterized
43	CAALFM_C307070CA	5.9226	2.70125E-54	Uncharacterized
44	CAALFM_C405900CA	5.9168	1.1249E-116	Uncharacterized
45	CAALFM_CR07260CA	5.8779	0.013967914	Uncharacterized
46	CAALFM_C106620CA	5.8775	0.016118237	Uncharacterized
47	CAALFM_C109300CA	5.8320	2.75478E-11	Uncharacterized
48	CAALFM_CR09530CA	5.7885	2.74225E-78	Uncharacterized
49	CAALFM_C209850CA	5.7740	3.08818E-07	Uncharacterized
50	CAALFM_C601940WA	5.5926	0.006011195	Uncharacterized

51	CAALFM_C100310WA	5.5729	6.50774E-57	Uncharacterized
52	CAALFM_C601810WA	5.5637	1.97617E-12	Uncharacterized
52	CAALFM_C110060CA	5.4134	4.01975E-08	Uncharacterized
54	CAALFM_CR07300WA	5.2272	7.10193E-05	Uncharacterized
55	CAALFM_C402330CA	5.2137	6.40082E-05	Uncharacterized
56	CAALFM_C603240WA	5.2105	9.75776E-08	Uncharacterized
57	CAALFM_C305840WA (FMO1)	5.1777	0.000145963	Uncharacterized

Table-3: List of top 100 downregulated genes in EDTA treated *C. albicans* cell (CAET)

Metabolic pathways No. of DEGs	**Name (44 DEGs)**	**Fold Change**	**FDR p-value**	**Function**
1	PHO100	100.3586958	1.7869E-210	encode an enzyme phosphomonoesterase
2	PLB1	75.16562361	3.7897E-221	Virulence; Phospholipase activity; Lipid metabolism
3	THI4	48.25803524	2.1564E-130	Involved in thiamine biosynthesis
4	THI13	25.45919657	8.2924E-175	Regulate IL-10 and IL-12 production
5	GIT1	22.7136005	3.2311E-112	functions as proton symporter
6	HSP31	18.09639	2.39778E-23	Involved in diauxic shift reprogramming
7	PHO84	17.26103731	4.3071E-163	High-affinity inorganic phosphate/H+ symporter
8	PUT1	14.48749801	7.5039E-99	Involved in amino acid metabolism
9	INO1	10.74384531	1.5532E-128	Encodes inositol-1-phosphate synthase
10	OPT1	10.46218378	1.83956E-90	Involved in peptide transportation
11	PUT2	8.132948215	1.989E-99	Amino acid metabolism regulator
12	LYS22	7.895086763	2.77628E-95	Homocitrate synthase activity and lysine auxotrophy
13	ACO2	7.333020332	2.21018E-91	Putative aconitate hydratase 2
14	SNZ1	7.225024726	2.98178E-78	Involved in pyridoxine (vitamin B6) synthesis
15	BTA1	7.201443893	2.2825E-11	Encodes the betaine lipid synthase
16	LYS4	6.846020558	1.77724E-70	Involve amino acid metabolism
17	CAN2	6.021560973	3.95846E-54	Import arginine
18	FCY24	5.986276905	4.80688E-58	Recruit vitamin B6 transport
19	THI6	5.891998871	3.5842E-104	Thiamine biosynthesis
20	LEU1	5.775957021	5.4161E-99	Catalyzes leucine biosynthesis pathway
21	GIS2	5.726657785	2.59522E-83	Encodes the homologue of mammalian CNBP

22	LYS12	5.682928227	1.2519E-72	Involved in dehydrogenation of homoisocitrate
23	CHA1	5.516083404	4.36052E-27	Involved in nutrient acquisition/metabolism
24	FET99	5.171473494	4.85608E-18	Involved in p-phenylenediamine oxidase; Iron transporter
25	GCV2	5.124244872	8.8508E-108	Catabolises glycine; Induction in elevated CO2
26	GIT3	4.705321982	1.43209E-52	Transport glycerophosphodiester metabolites into cells
27	CYC1	4.533120319	7.41108E-12	Encode cytochrome c
28	HXT5	4.370444946	3.87863E-30	Uptake fructose, glucose and mannose
29	ILV3	4.326855778	2.72309E-49	Amino acid metabolism regulator
30	OPT3	4.085475749	1.8761E-38	Transport of sulfur-containing compounds
31	GAL1	4.015748921	6.75558E-71	Executes metabolic functions in carbon source uptake
32	GCY1	3.986027968	4.12996E-66	Confers hypersensitivity to toxic ergosterol analog
33	GAL10	3.818893745	1.55917E-65	Induce biofilm; Utilize the source of galactose
34	GDH2	3.769049401	8.49692E-47	Catalyzes deamination of glutamate to alpha-ketoglutarate
35	GCV1	3.737254451	2.09928E-39	Catabolises glycine; Induction in elevated CO2
36	DFR1	3.498716699	3.23053E-05	Catalyses of 7,8-dihydrofolate to 5,4,7,8-tetrahydrofolate
37	GDH3	3.475852592	9.07648E-30	Encode NADP+-dependent glutamate dehydrogenases
38	CTP1	3.456185992	2.97824E-16	Involved in transportion of citrate
39	TPO4	3.351032169	4.97048E-29	Bcr1- associated repression in RPMI a/alpha biofilms
40	OPI3	3.327563871	1.89288E-15	Biosynthesis of phosphatidylcholine
41	EGD2	3.290389697	2.54237E-30	GlcNAc-induced protein
42	LYS2	3.228201144	3.15144E-40	lysine biosynthesis; biofilm induced
43	NUP	3.137825901	7.10193E-05	Involved in transportion of purine nucleosides and thymidine
44	ARO3	3.04435509	1.66463E-45	aromatic amino acid synthesis;
Cell-wall associated				
	Name (7 DEGs)	**Fold Change**	**FDR p-value**	**Function**
1	HGT2	22.87250932	1.9154E-170	Encode cell- wall associated proteins
2	PGA10	9.817718799	2.80343E-96	Involved in Iron acquisition
3	TRY6	8.936709002	5.07311E-24	Transcriptional regulator in biofilm
4	HSP30	6.401066175	8.86109E-17	Stress-protective function on plasma

				membrane
5	ECM331	3.900822094	5.76083E-24	Involved in cell wall biogenesis
6	ACS2	3.097921844	3.19601E-24	antigenic during human and murine infection
7	STB3	3.038270294	5.50968E-41	caspofungin induced
Ribosomal				
	Name (13 DEGs)	**Fold Change**	**FDR p-value**	**Function**
1	RPS28B	5.090570767	1.40419E-10	Autoregulates the decapping of its own mRNA machinery
2	RPS42	4.347730989	1.02472E-32	Enhance tolerance to fluconazole
3	RDN18	4.047975479	1.9867E-13	component of the small (40S) ribosomal subunit;
4	RPS12	3.944266266	1.51774E-29	pre-rRNA processing and polysome content
5	RPP1B	3.606949912	2.33237E-25	Involved in regulation of translation elongation
6	RPS21B	3.588439098	1.10333E-29	Regulated by Nrg1, Tup1
7	RPS13	3.497233295	3.88662E-35	_
8	ASC1	3.385291153	3.46635E-25	Required for virulence in mice
9	RPL18	3.234852275	1.52941E-28	repressed upon phagocytosis by murine macrophage
10	RPL9B	3.193159155	3.27531E-29	repressed upon phagocytosis by murine macrophages
11	RPL5	3.102732401	2.25382E-30	repressed upon phagocytosis by murine macrophages
12	RPP2B	3.083956604	5.93521E-16	possibly involved in regulation of translation elongation
13	RPS27	3.03019245	2.15647E-21	repressed upon phagocytosis by murine macrophage
Others	**Name (11 DEGs)**	**Fold Change**	**FDR p-value**	**Function**
1	PGA45	5.590917256	6.40747E-43	Putative GPI-anchored protein of unknown function
2	RBT7	4.226949465	1.5772E-09	Encode secreted RNase T2
3	PEX4	3.972508718	1.24715E-12	Spider biofilm induction
4	RME1	3.697681605	7.1604E-68	Development of fluconazole resistance
5	THI20	3.271494397	5.58989E-53	Spider biofilm induced
6	ASM3	3.235903328	1.59858E-31	Possible Kex2 substrate
7	BFR1	3.226066337	1.87417E-16	Protein involved in the maintenance of normal ploidy
8	TUF1	3.224254282	7.29461E-36	Encodes GTPase mitochondrial elongation factor Tu

9	GAL7	3.207467422	7.9819E-49	downregulated by hypoxia
10	SSP96	3.203024284	1.12259E-06	F-12/CO2 early biofilm induced
11	CYB5	3.179133812	1.7903E-06	induced in high iron
Uncharacterized				
	Name (25 DEGs)	**Fold Change**	**FDR p-value**	**Function**
1	CAALFM_C400530CA	25.251715	3.77714E-07	Uncharacterized
2	CAALFM_CR08830WA	13.160107	3.7788E-05	Uncharacterized
3	CAALFM_CR06430WA	6.746508	0.002469228	Uncharacterized
4	CAALFM_CR09350CA	6.189599	1.40099E-55	Uncharacterized
5	CAALFM_C112940CA	6.061342	0.037846274	Uncharacterized
6	CAALFM_C404230WA	5.563465	2.28386E-82	Uncharacterized
7	CAALFM_C106870CA	5.0202	0.017180492	Uncharacterized
8	CAALFM_C306240CA (MRPL39)	4.970367	0.002579226	Uncharacterized
9	CAALFM_C500130CA (YML34)	4.786879	5.51407E-07	Uncharacterized
10	CAALFM_C204770WA	4.55791	0.001066926	Uncharacterized
11	CAALFM_C103620CA	4.161708	4.50987E-09	Uncharacterized
12	CAALFM_C501540WA (RPS11A)	3.909799	3.0519E-17	Uncharacterized
13	CAALFM_C503290CA (MRP10)	3.907568	1.74642E-10	Uncharacterized
14	CAALFM_C503480CA	3.871642	1.41077E-32	Uncharacterized
15	CAALFM_C208180CA	3.782614	0.001381795	Uncharacterized
16	CAALFM_C400990WA	3.6619335	0.000850431	Uncharacterized
17	CAALFM_C403500CA	3.65632	0.012820924	Uncharacterized
18	CAALFM_C204110WA	3.438488	1.6049E-10	Uncharacterized
19	CAALFM_C703560WA	3.37104	3.35062E-18	Uncharacterized
20	CAALFM_C108770WA	3.243523	1.51784E-29	Uncharacterized
21	CAALFM_CR03110WA (MSE1)	3.172182	6.38954E-14	Uncharacterized
22	CAALFM_CR03470WA	3.162178	2.39698E-48	Uncharacterized
23	CAALFM_CR08480CA (RPS29A)	3.142855	2.18259E-06	Uncharacterized
24	CAALFM_CR02380CA	3.093999	0.000634778	Uncharacterized
25	CAALFM_C400230WA	3.0457946	8.36614E-08	Uncharacterized

1

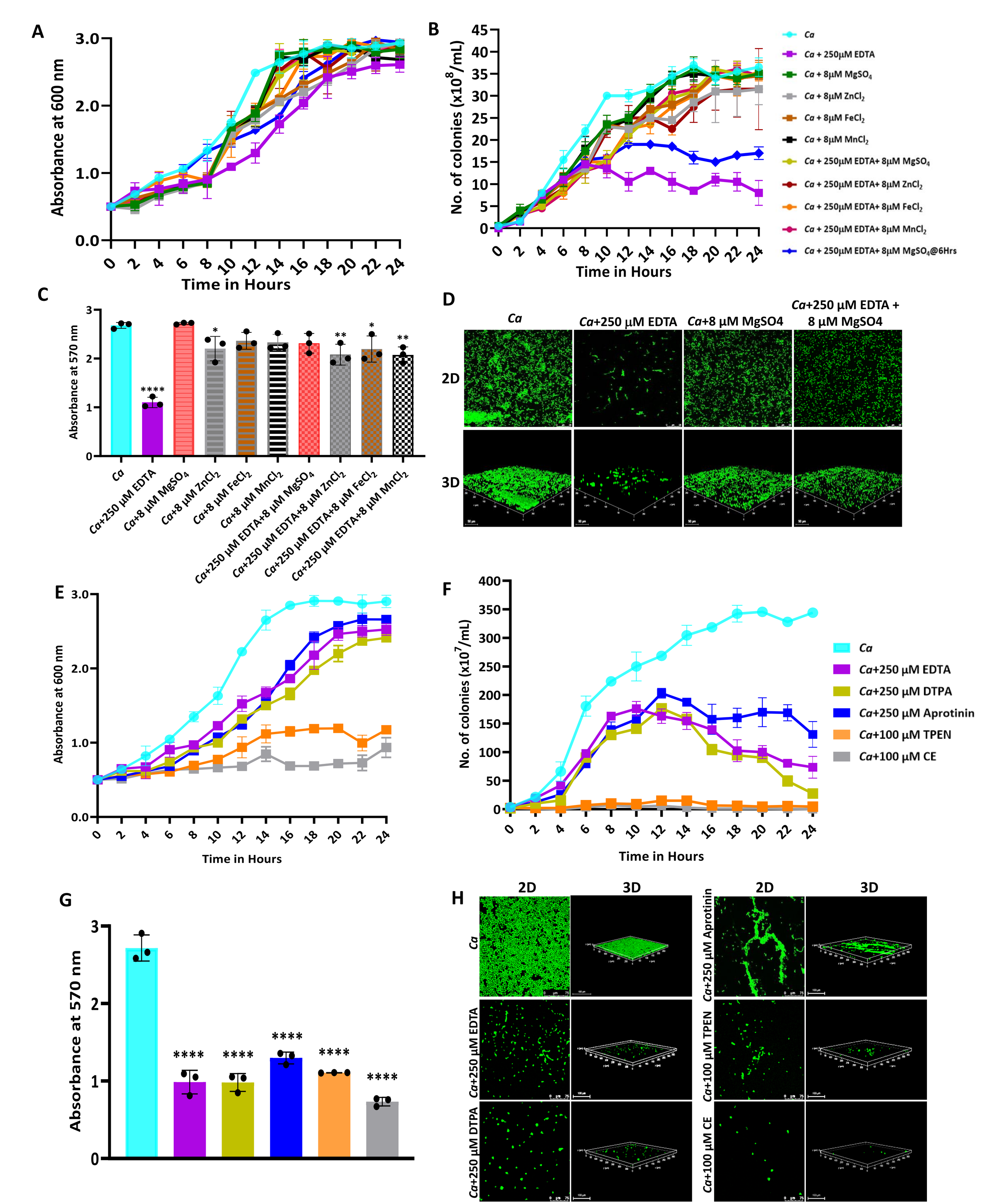
A
Absorbance at 600 nm
Time in Hours
B
No. of colonies (x10^8/mL)
Time in Hours
Ca
Ca + 250µM EDTA
Ca + 8µM MgSO4
Ca + 8µM ZnCl2
Ca + 8µM FeCl2
Ca + 8µM MnCl2
Ca + 250µM EDTA+ 8µM MgSO4
Ca + 250µM EDTA+ 8µM ZnCl2
Ca + 250µM EDTA+ 8µM FeCl2
Ca + 250µM EDTA+ 8µM MnCl2
Ca + 250µM EDTA+ 8µM MgSO4@6Hrs
C
Absorbance at 570 nm
Ca
Ca+250 µM EDTA
Ca+8 µM MgSO4
Ca+8 µM ZnCl2
Ca+8 µM FeCl2
Ca+8 µM MnCl2
Ca+250 µM EDTA+8 µM MgSO4
Ca+250 µM EDTA+8 µM ZnCl2
Ca+250 µM EDTA+8 µM FeCl2
Ca+250 µM EDTA+8 µM MnCl2
D
Ca
Ca+250 µM EDTA
Ca+8 µM MgSO4
Ca+250 µM EDTA + 8 µM MgSO4
2D
3D
E
Absorbance at 600 nm
Time in Hours
F
No. of colonies (x10^7/mL)
Time in Hours
Ca
Ca+250 µM EDTA
Ca+250 µM DTPA
Ca+250 µM Aprotinin
Ca+100 µM TPEN
Ca+100 µM CE
G
Absorbance at 570 nm
H
2D
3D
Ca
Ca+250 µM EDTA
Ca+250 µM DTPA
Ca+250 µM Aprotinin
Ca+100 µM TPEN
Ca+100 µM CE

Figure 1

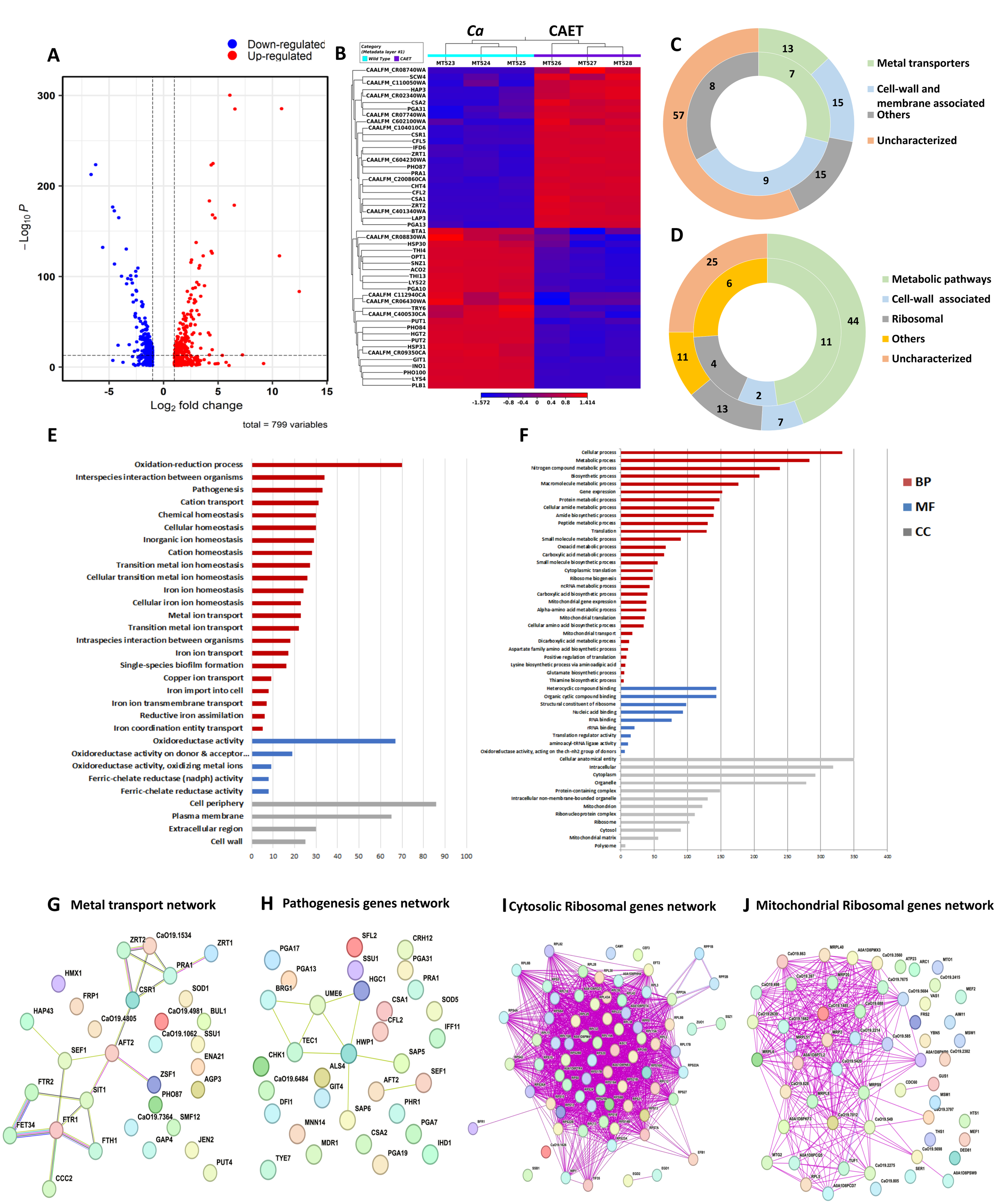
A
Down-regulated
Up-regulated
$-Log_{10}$ P
Log_2 fold change
total = 799 variables
B
Ca
CAET
MT523
MT524
MT525
MT526
MT527
MT528
C
Metal transporters
Cell-wall and membrane associated
Others
Uncharacterized
D
Metabolic pathways
Cell-wall associated
Ribosomal
Others
Uncharacterized
E
Oxidation-reduction process
Interspecies interaction between organisms
Pathogenesis
Cation transport
Chemical homeostasis
Cellular homeostasis
Inorganic ion homeostasis
Cation homeostasis
Transition metal ion homeostasis
Cellular transition metal ion homeostasis
Iron ion homeostasis
Cellular iron ion homeostasis
Metal ion transport
Transition metal ion transport
Intraspecies interaction between organisms
Iron ion transport
Single-species biofilm formation
Copper ion transport
Iron import into cell
Iron ion transmembrane transport
Reductive iron assimilation
Iron coordination entity transport
Oxidoreductase activity
Oxidoreductase activity on donor & acceptor...
Oxidoreductase activity, oxidizing metal ions
Ferric-chelate reductase (nadph) activity
Ferric-chelate reductase activity
Cell periphery
Plasma membrane
Extracellular region
Cell wall
F
BP
MF
CC
G Metal transport network
H Pathogenesis genes network
I Cytosolic Ribosomal genes network
J Mitochondrial Ribosomal genes network

Figure 2

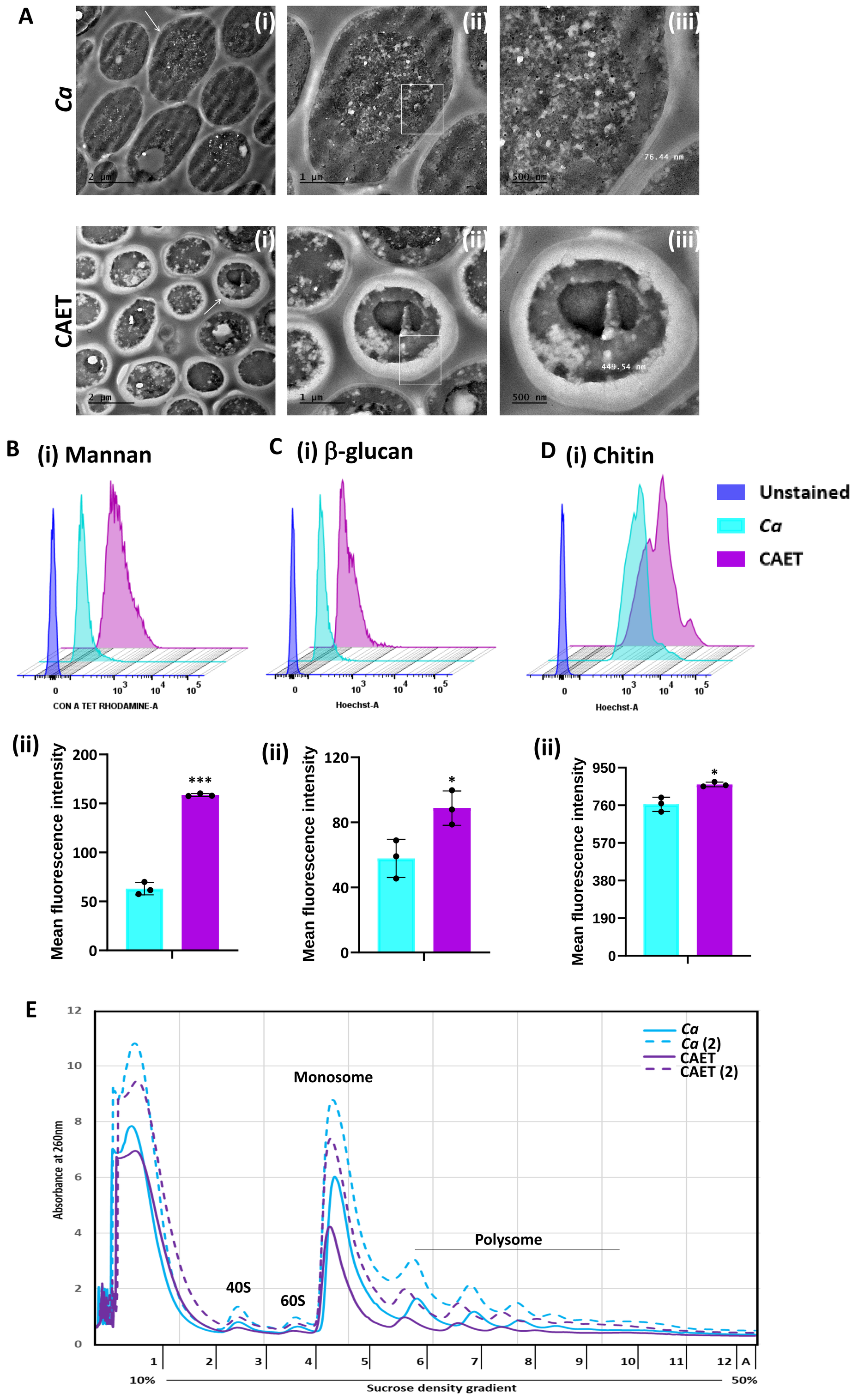
A
Ca
CAET
(i)
(ii)
(iii)
2 µm
1 µm
500 nm
76.44 nm
449.54 nm
B (i) Mannan
C (i) β-glucan
D (i) Chitin
Unstained
Ca
CAET
CON A TET RHODAMINE-A
Hoechst-A
(ii)
Mean fluorescence intensity
***
*
E
Absorbance at 260nm
Monosome
Polysome
40S
60S
Ca
Ca (2)
CAET
CAET (2)
10%
50%
Sucrose density gradient

Figure 3

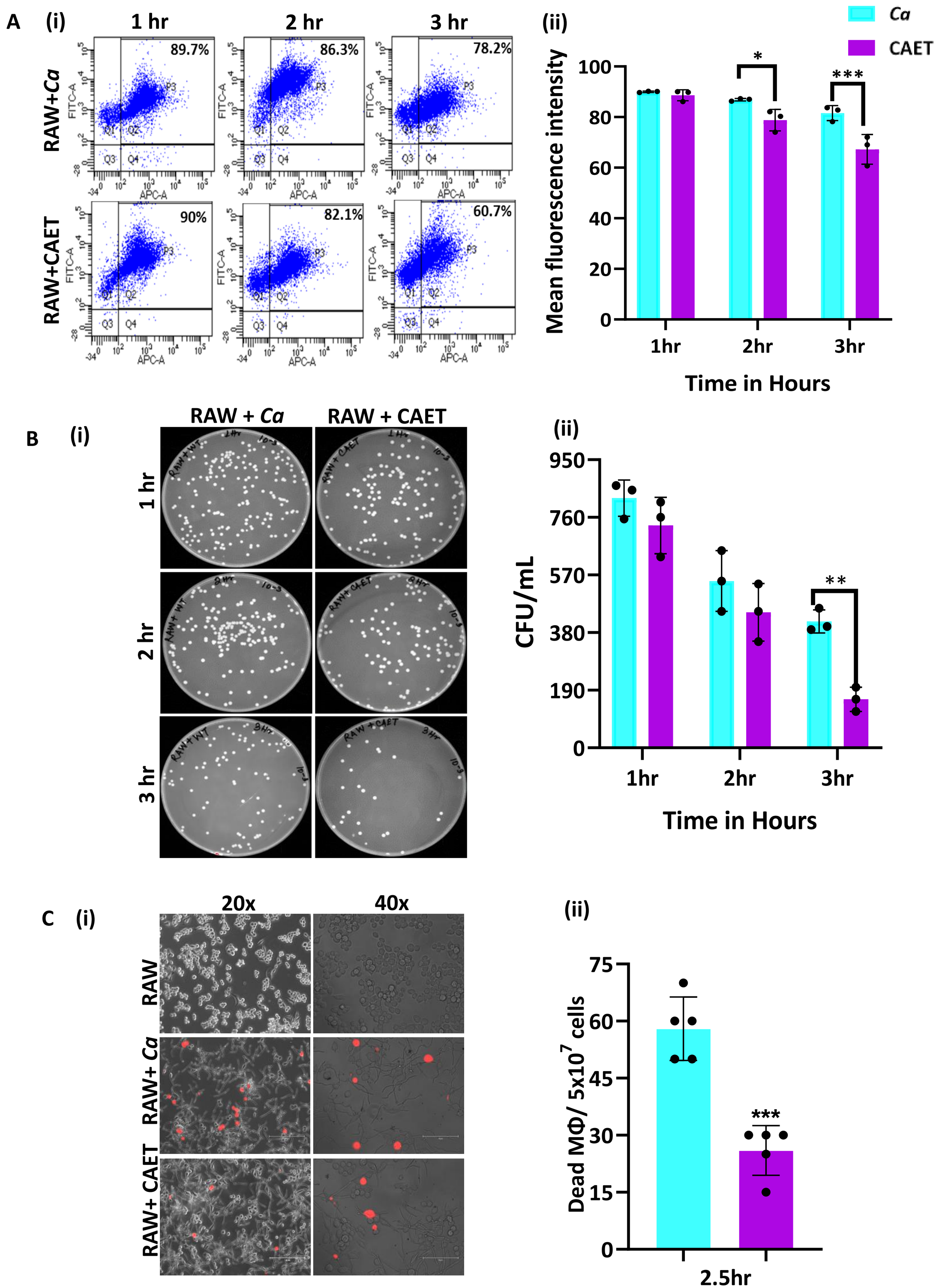
A
(i)
1 hr
2 hr
3 hr
RAW+Ca
RAW+CAET
89.7%
86.3%
78.2%
90%
82.1%
60.7%
FITC-A
APC-A
(ii)
Ca
CAET
Mean fluorescence intensity
100
80
60
40
20
0
*
***
1hr
2hr
3hr
Time in Hours
B
(i)
RAW + Ca
RAW + CAET
1 hr
2 hr
3 hr
(ii)
CFU/mL
950
760
570
380
190
0
**
1hr
2hr
3hr
Time in Hours
C
(i)
20x
40x
RAW
RAW+ Ca
RAW+ CAET
(ii)
Dead MΦ/ 5x10^7 cells
75
60
45
30
15
0
***
2.5hr

Figure 4

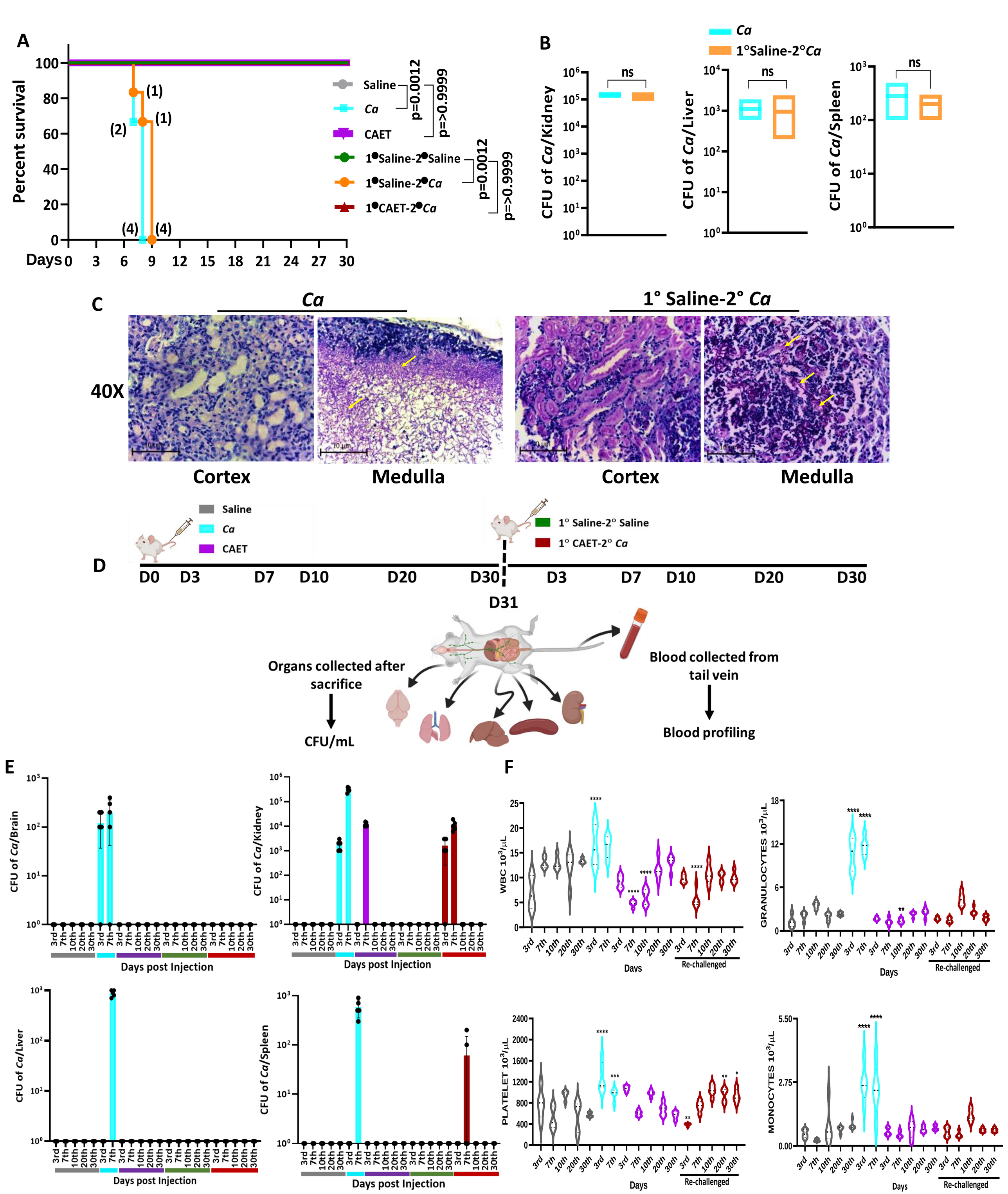
A
Percent survival
Days
Saline
Ca
CAET
1●Saline-2●Saline
1●Saline-2●Ca
1●CAET-2●Ca
p=0.0012
p=>0.9999
B
Ca
1°Saline-2°Ca
ns
CFU of Ca/Kidney
CFU of Ca/Liver
CFU of Ca/Spleen
C
Ca
1° Saline-2° Ca
40X
Cortex
Medulla
D
Saline
Ca
CAET
1° Saline-2° Saline
1° CAET-2° Ca
D0
D3
D7
D10
D20
D30
D31
Organs collected after sacrifice
CFU/mL
Blood collected from tail vein
Blood profiling
E
CFU of Ca/Brain
CFU of Ca/Kidney
CFU of Ca/Liver
CFU of Ca/Spleen
Days post Injection
F
WBC 10³/μL
GRANULOCYTES 10³/μL
PLATELET 10³/μL
MONOCYTES 10³/μL
Days
Re-challenged

Figure 5

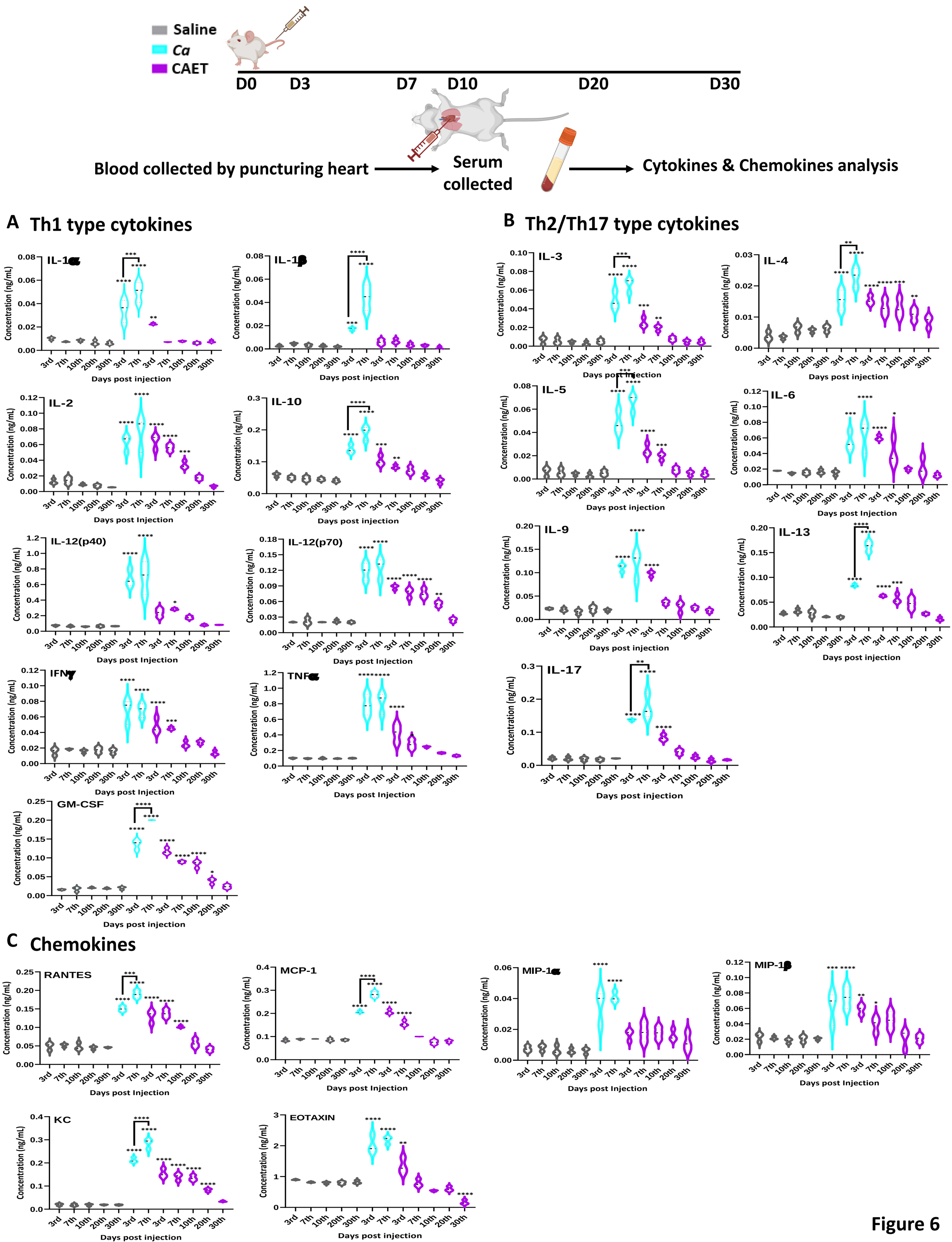
Saline
Ca
CAET
D0
D3
D7
D10
D20
D30
Blood collected by puncturing heart
Serum collected
Cytokines & Chemokines analysis
A Th1 type cytokines
IL-1α
IL-1β
IL-2
IL-10
IL-12(p40)
IL-12(p70)
IFNγ
TNFα
GM-CSF
B Th2/Th17 type cytokines
IL-3
IL-4
IL-5
IL-6
IL-9
IL-13
IL-17
C Chemokines
RANTES
MCP-1
MIP-1α
MIP-1β
KC
EOTAXIN
Concentration (ng/mL)
Days post injection
3rd
7th
10th
20th
30th

Figure 6

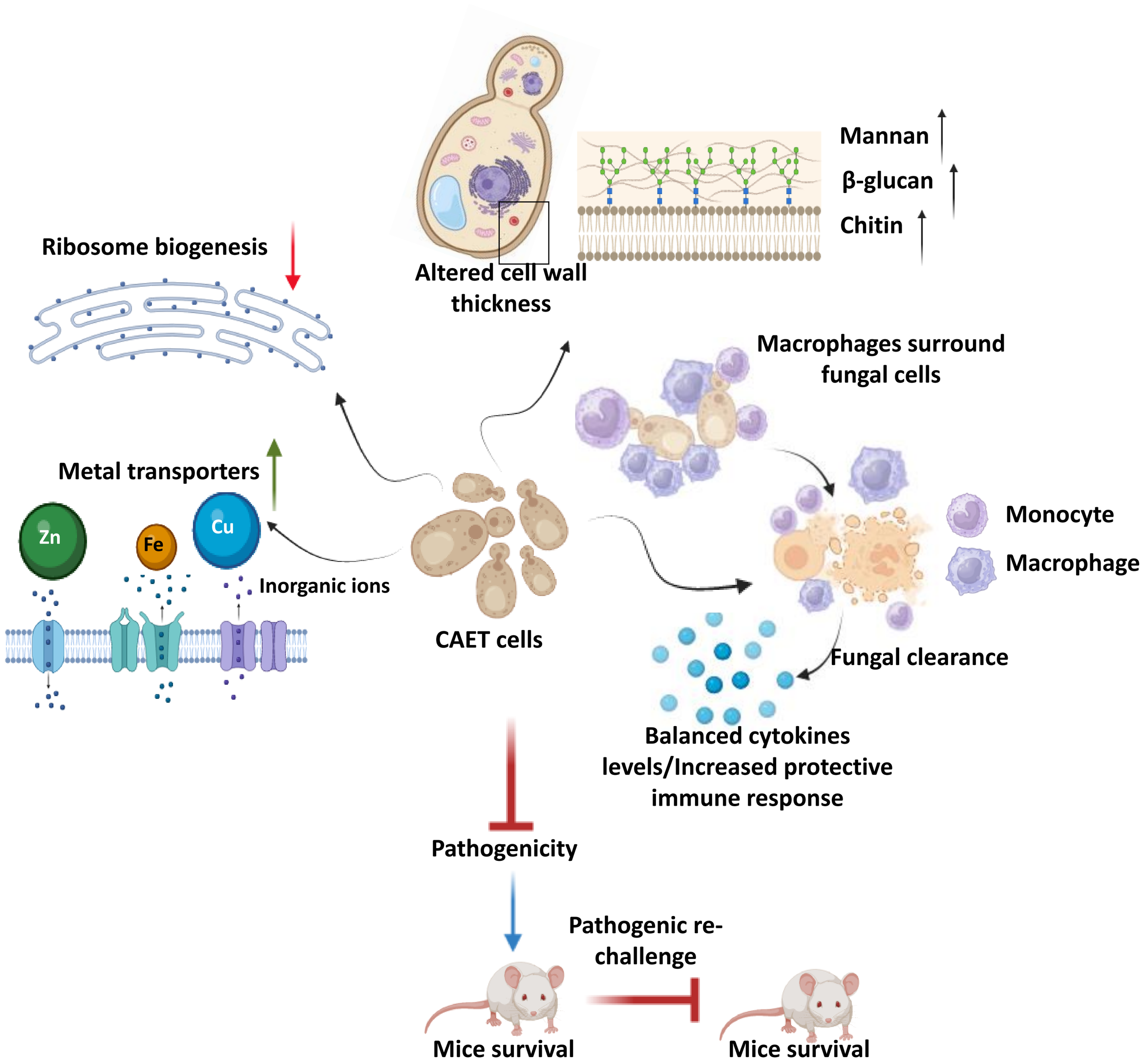
Mannan
β-glucan
Chitin
Altered cell wall thickness
Ribosome biogenesis
Macrophages surround fungal cells
Metal transporters
Zn
Fe
Cu
Inorganic ions
CAET cells
Monocyte
Macrophage
Fungal clearance
Balanced cytokines levels/Increased protective immune response
Pathogenicity
Pathogenic re-challenge
Mice survival
Mice survival

Figure 7